1.0

1.1

1.25   1.4   1.6

2.8   2.5
3.2   2.2
3.6
4.0   2.0

1.8

MICROCOPY RESOLUTION TEST CHART
NATIONAL BUREAU OF STANDARDS-1963-A

ADA037011

DESIGN CURVES FOR STRUCTURAL RESPONSE
DUE TO IMPACT LOADING

BY

Pei Chi Chou and William J. Flis

DREXEL UNIVERSITY

Philadelphia, Pennsylvania 19104

October 1976

FINAL REPORT

(July 1975 to June 1976)

Prepared for

Air Vehicle Technology Department

NAVAL AIR DEVELOPMENT CENTER

Warminster, Pennsylvania 18974

(18) (19) REPORT DOCUMENTATION PAGE		READ INSTRUCTIONS BEFORE COMPLETING FORM
1. REPORT NUMBER NADC 76380-30	2. GOVT ACCESSION NO.	3. RECIPIENT'S CATALOG NUMBER
4. TITLE (and Subtitle) Design Curves for Structural Response due to Impact Loading,		5. TYPE OF REPORT & PERIOD COVERED Final Contract Report, July 1975 — June 1976
		6. PERFORMING ORG. REPORT NUMBER
7. AUTHOR(s) Pei Chi Chou and William J. Flis		8. CONTRACT OR GRANT NUMBER(s) N62269-75-C-0425
9. PERFORMING ORGANIZATION NAME AND ADDRESS Drexel University 32nd and Chestnut Streets Philadelphia, Pa. 19104		10. PROGRAM ELEMENT, PROJECT, TASK AREA & WORK UNIT NUMBERS
11. CONTROLLING OFFICE NAME AND ADDRESS		12. REPORT DATE October 1976
		13. NUMBER OF PAGES 76
14. MONITORING AGENCY NAME & ADDRESS(If different from Controlling Office)		15. SECURITY CLASS. (of this report) UNCLASSIFIED
		15a. DECLASSIFICATION/DOWNGRADING SCHEDULE

16. DISTRIBUTION STATEMENT (of this Report)

Approved for public release; distribution unlimited.

17. DISTRIBUTION STATEMENT (of the abstract entered in Block 20, if different from Report)

D D C
MAR 16 1977
C

18. SUPPLEMENTARY NOTES

19. KEY WORDS (Continue on reverse side if necessary and identify by block number)

Impact
Structural Response
Composite Materials

20. ABSTRACT (Continue on reverse side if necessary and identify by block number) A method is developed to produce a design curve for predicting the response of a given type of structure to impact loading. This curve gives the maximum strain in the structure, which may have various size and material properties, due to impacts involving different masses and velocities. An example of a simply supported beam under central impact is presented in detail. Both experimental results and numerical calculations were used in establishing the design curve. This curve implies that, for large impactor masses, the controlling parameter is the ratio of structural to impactor mass; the strain is linearly proportional to impact velocity and inversely proportional to the square root of the mass ratio.

DD FORM 1 JAN 73 1473 EDITION OF 1 NOV 65 IS OBSOLETE
S/N 0102-014-6601

405723

Table of Contents

1

Foreword

This is the final technical report of Contract No.N62269-75-C-0425, sponsored by the Naval Air Development Center, Warminster, Pa. The work was performed during the period July 1, 1975 through June 30, 1976. Mr. Lee Gause was the contract monitor.

Part of the contents of this report has been presented in a paper entitled "Design Curves for Structural Response Due to Impact Loading," at the AIAA/ASME/SAE 17th Structures, Structural Dynamics, and Materials Conference, held at King of Prussia, Pa., May 5-7, 1976. A synoptic of this paper, entitled "Design Curves for Beams under Impact Loading," has been accepted for publication in the AIAA Journal.

The authors would like to express thanks to Dr. Edward J. McQuillen, Dr. James L. Huang, and Mr. Lee W. Gause of the Naval Air Development Center for their support and suggestions and to Mr. Frank Patota and Mr. Donald Rosen of Drexel University for performing the experiments.

2

I. Introduction

Aerospace structures are often subjected to impact loadings, including foreign objects entering jet engines, and dropped tools, hail, and runway stones impinging on exposed aircraft components. For impacts by blunt objects at moderate velocities, the failure of the impacted structure is usually of the "structural" type, rather than local perforation or contact failure. This report deals with the structural type of transient response due to impact loadings.

Because of the complicated geometry of most structures, the calculation of transient response by the usual finite-element computer codes can be very tedious and time-consuming. At present, there are no satisfactory methods for convenient calculation of the maximum transient stress or strain; designers need a simple method for this purpose.

In this report we develop a method to generate a single design curve for a given type of structure. This curve gives the maximum strain in the structure, which may have various dimensions and material properties, due to impacts of different values of mass and velocity. As an example, a design curve for a simply supported beam under a central transverse impact is presented. It is shown that a single curve of a generalized strain $\bar{\varepsilon}$ versus the ratio M of beam mass to impactor mass can represent many impact situations. This curve may be generated by theoretical calculations with different degrees of sophistication, or by a limited number of experiments.

In the development of the design curve, we have studied six analytical models for treating beam impact response. Three of these are lumped-parameter models consisting of masses and springs; the other three are distributed-mass models, which take the beam vibration modes into consideration. Some of these models neglect the contact force and treat the beam with the attached impactor mass as a free transient-vibration problem. Other models include the contact force term, trace the impactor motion distinctly, and treat the beam as a forced-vibration problem. It will be shown that for the models neglecting the contact force, the generalized strain $\bar{\epsilon}$ is a function of mass ratio M only and is independent of other parameters. For the two models which include the contact force, $\bar{\epsilon}$ depends on M and other parameters, but the dependence on these other parameters is weak, and a single $\bar{\epsilon}$ vs. M curve can still give an approximate representation of all impact situations.

A series of impact experiments has been conducted using beams of various materials and dimensions and a range of impactor masses and velocities. By plotting the results in the $\bar{\epsilon}$ versus M plane, a single curve can again be drawn through all data points, with approximately $\pm$ 30% deviation.

In constructing such a curve for design purposes, it is suggested that a particular analytical model be chosen for calculation, this selection to be based on the amount and reliability of the information desired, the particular properties of the structure (e.g., damping, plastic behavior), availability of computing facilities, etc. Alternatively, a limited number of impact experiments can be conducted. Regardless of whether an analytical calculation or a series of experiments is used, the results can be plotted as an $\bar{\epsilon}$ vs. M curve, which can then be applied to predict impact behavior for all impact situations within the considered range of values of M.

4

The analytical models and methods discussed here are applicable to all values of M, so that for a given beam, the impactor mass may be large or small. The proposed design curve presented here, however, is limited to small values of M, or large impactor masses. Some other nondimensional parameters may have to be developed to treat fully, impacts by small impactor masses. For structures other than a simply supported beam, a similar method can be used to construct the design curve.

II. Analytical Solutions of Beam Impact

There have been many analytical derivations for beam response due to transverse central impact. Most of these are presented in the excellent book by Goldsmith [1].

In order to develop a practical design curve, we have performed numerical calculations by many of these existing methods, and also by some new methods or extensions of existing methods. In the following we shall review the basic approach of each and present the numerical results. In all cases, the problem treated is the midspan impact of a simply supported beam.

Table I gives an index to the six analytical models to be discussed. As can be seen, three of these are lumped-mass models and three are continuous-mass models.

1. One-Degree-of-Freedom, Energy-Conserved Model

If we are only interested in the maximum deflection and strain in the beam, and not their complete spatial and temporal distributions, a simple one-degree-of-freedom model with a lumped mass and spring is most convenient. Either one of two different basic assumptions can be adopted; the first conserves the energy but not the momentum, the second just the opposite.

5

In the energy-conserved model, it is assumed that the spatial distribution of the beam deflection is identical to the static deflection of the beam loaded by a concentrated force. By equating the original kinetic energy with the static strain energy in the beam, the maximum deflection can be determined. In other words, only one vibration mode is considered, with mode shape the same as the static deflection curve. This model may be depicted by a spring with constant K_1 impacted by a mass m_2 at a velocity v, as shown in Fig. (1). From the static beam deflection formula $\delta = (PL^3/48EI)$, it is evident that

$$K_1 = 48EI/L^3 \tag{1}$$

The maximum deflection of the spring-mass system with initial velocity v is then

$$w_{1_{max}} = v\sqrt{\frac{m_2}{K_1}} \tag{2}$$

This equation was first derived by Young [2] and is also presented in [1]. We shall now extend this approach to obtain the maximum strain in the beam. The static deflection of the beam is

$$w(x) = w_1 \frac{x}{L}\left[3 - \frac{4x^2}{L^2}\right], \qquad 0 < x < \frac{L}{2} \tag{3}$$

where w_1 is the deflection at midspan. The maximum strain, which occurs also at $x = L/2$, is then

6

$$\varepsilon_{max} = -\frac{h}{2} \frac{\partial^2 w}{\partial x^2}\bigg|_{x=L/2} = \frac{6h}{L^2} w_{1_{max}} \tag{4}$$

where we have replaced the static w_1 by $w_{1_{max}}$. Substituting Eq. (2) into Eq. (4), and introducing the definition of generalized strain

$$\bar{\varepsilon} = \varepsilon_{max} \ (a^2/hv) \tag{5}$$

we obtain

$$\bar{\varepsilon} = \sqrt{\frac{3}{4M}} \tag{6}$$

Note that the generalized strain $\bar{\varepsilon}$ is a function of the mass ratio M only. This equation may be plotted as an $\bar{\varepsilon}$ vs. M curve and will be discussed later.

It is also interesting to note that the final result of this model is independent of the beam mass, as long as the total energy is conserved. For instance, considering the model as shown in Fig. 2, with the beam mass equal to m_1 (or any other value), then, if the kinetic energy of the impactor is equated with the initial kinetic energy of the combined mass $m_1 + m_2$, the combined mass will have an initial velocity

$$v_0 = \sqrt{\frac{m_2}{(m_1 + m_2)}} \ v \ . \tag{7}$$

Assuming m_1 and m_2 are subsequently traveling at the same velocity after initial contact, then the maximum deflection is also given by Eq. (2). It is recognized that Eq. (7) violates the conservation of momentum; if no energy is dissipated, the impact is elastic, and the impactor will rebound. It will be shown later that due to multiple sub-impacts, Eq. (7) is still a good assumption for calculating final deflection and strain.

2. One-Degree-of-Freedom, Momentum-Conserved Model

This model conserves the initial momentum but not the initial kinetic energy.   Refer to Figure 2 where the beam is replaced by an equivalent mass $(17/35)m_1$ and an equivalent spring constant K_1. The expression for the equivalent mass is obtained by matching the kinetic energy of the equivalent mass traveling at the velocity of the beam midspan point, and the kinetic energy of the beam, assuming that the deflection mode shape is the static deflection curve. If the initial impact is perfectly inelastic, then momentum conservation yields

$$m_2 v = (m_2 + \frac{17}{35} m_1)v_0 \tag{8}$$

or

$$v_0 = v/(1 + \frac{17}{35} M) \tag{9}$$

After the initial impact, the two masses are attached and undergo a free vibration with initial velocity v_0 given by Eq. (9). The maximum deflection is then

$$w_{1_{max}} = v_0 \sqrt{\frac{m_2(1 + \frac{17}{35} M)}{K_1}} \tag{10}$$

This result is known as the Cox equation [1], [3]. We shall now extend it to give the maximum strain. Following the approach used in the previous case, Eqs. (4), (5) and (10) may be combined to yield

$$\bar{\varepsilon} = \left[\frac{3}{4M(1 + 17M/35)} \right]^{1/2} \tag{11}$$

This expression gives lower values of $\bar{\varepsilon}$ as compared to the energy-conserved case, Eq. (6). For small values of M, Eq. (11) approaches Eq. (6).

8

3. Two-Degrees-of-Freedom Model

In the one-degree-of-freedom models considered above, the contact force and relative motion between the impactor and the beam are neglected. As a result, either conservation of momentum or conservation of energy must be violated, and the impactor is always attached to the beam, allowing no rebound or multiple sub-impacts. The simplest way to include the contact force is to consider the impactor as a separate rigid body and account for its motion, leading to a two-degrees-of-freedom model.

According to the Hertzian contact principle, the contact force F is related to the "approach", or relative displacement α, by the relation

$$F = k_2 \, \alpha^{3/2} \tag{12}$$

which is nonlinear. For simplicity, we shall approximate this relation by a linear one,

$$F = K_2 \, \alpha \ . \tag{13}$$

The constant K_2 can be adjusted to give a good approximation to Eq. (12) for a given impact, as shown in Fig. 3. Further, in order to allow for multiple sub-impacts, this spring is limited to resist only compression; that is, the force in the spring is

$$F = \begin{cases} K_2 \, \alpha, & \text{for } \alpha \geq 0 \\ 0, & \text{for } \alpha < 0 \end{cases} \tag{14}$$

Note that the beam and impactor are in contact only when $\alpha \geq 0$.

9

The equations of motion of this system (Fig. 4) are then

$$\left.\begin{array}{r} \frac{17}{35} m_1 \ddot{w}_1 + (K_1 + K_2)w_1 - K_2 w_2 = 0 \\ m_2 \ddot{w}_2 + K_2(w_2 - w_1) = 0 \end{array}\right\} \quad \text{for } \alpha \geq 0 \qquad (15)$$

while the beam and impactor are in contact. During periods when the two are separated, the beam vibrates freely, so that

$$\left.\begin{array}{r} \frac{17}{35} m_1 \ddot{w}_1 + K_1 w_1 = 0 \\ \ddot{w}_2 = 0 \end{array}\right\} \quad \text{for } \alpha < 0 \qquad (16)$$

The second condition corresponds to free flight of the impactor. Using the initial conditions

$$w_1(0) = w_2(0) = 0$$

$$\dot{w}_1(0) = 0$$

$$\dot{w}_2(0) = v$$

we can obtain a solution of the above equations, as detailed in Appendix A.

Having determined the motion of the beam $w_1(t)$, the maximum value of the deflection $w_{1_{max}}$ may be substituted into Eqs. (4) and (5), yielding a corresponding value of $\bar{\epsilon}$ which is then plotted as one point in the $\bar{\epsilon}$ vs. M diagram, Fig. 5. It is demonstrated in Appendix A that $\bar{\epsilon}$, so obtained, is a function of $M = m_1/m_2$ and $K = K_1/K_2$ only, and that its dependence on the stiffness ratio K is weak for realistic values of K_1 and K_2. In other words, $\bar{\epsilon}$ does not change much as the value of K is varied. Therefore, only one curve is shown in Fig. 5 for the two-degrees-of-freedom model.

10

4. Clebsch Solution

A solution of the beam impact problem which considers the vibrations of the distributed mass of the beam was first introduced by Clebsch and subsequently presented by St. Venant [1], [4]. The impactor mass is considered as rigid and attached to the beam at the impact point. An initial velocity equal to the original impactor velocity is assumed at the beam point where the impactor mass is attached. The subsequent free vibration of the beam is then solved.

The Euler-Bernoulli beam equation is used

$$EI \frac{\partial^4 w}{\partial x^4} + \rho A \frac{\partial^2 w}{\partial t^2} = 0 \qquad (17)$$

where w is the deflection of the beam. The boundary conditions for impact at beam midspan are

$$w(0,t) = \frac{\partial^2 w}{\partial x^2}(0,t) = \frac{\partial w}{\partial x}\left(\frac{L}{2},t\right) = 0 \qquad (18)$$

$$EI \frac{\partial^3 w}{\partial x^3}(L/2,t) = (1/2)m_2 \frac{\partial^2 w}{\partial t^2}(L/2,t). \qquad (19)$$

The last condition equates the shear force at midspan of the beam with the inertia force of the impactor m_2, and implies that the beam and impactor are always in contact (perfectly inelastic impact). Note that local contact deformation is neglected and that the impactor is rigid.

11

The initial conditions are

$$\begin{cases} \dfrac{\partial w}{\partial t} = 0 & \text{for } t = 0, \ x \neq L/2 \\[2mm] \dfrac{\partial w}{\partial t} = v_2 & \text{for } t = 0, \ x = L/2 \end{cases} \tag{20}$$

$$w(x,0) = 0 \tag{21}$$

The beam equation (17), together with the boundary conditions Eqs. (18) and (19), and the initial conditions Eqs. (20) and (21), are solved, with the resulting deflection

$$w = \frac{L^2 v}{a^2} \sum_{i=1}^{\infty} \frac{1}{\phi_i^3} \frac{\dfrac{\sin \dfrac{2\phi_i x}{L}}{\cos \phi_i} - \dfrac{\sinh \dfrac{2\phi_i x}{L}}{\cosh \phi_i}}{\dfrac{1}{\cos^2 \phi_i} - \dfrac{1}{\cosh^2 \phi_i} + \dfrac{2M}{\phi_i^2}} \sin \frac{4\phi_i^2 a^2}{L^2} t \tag{22}$$

where ϕ_i is the eigenvalue to be solved from the equation

$$\phi_i (\tan \phi_i - \tanh \phi_i) = 2M \ .$$

The maximum strain along the length of the beam occurs at $x = L/2$, and is

$$\varepsilon = - \frac{4z \, v}{a^2} \sum_{i=1}^{\infty} \frac{1}{\phi_i} \frac{\tan \phi_i + \tanh \phi_i}{\dfrac{1}{\cos^2 \phi_i} - \dfrac{1}{\cosh^2 \phi_i} + \dfrac{2M}{\phi_i^2}} \sin \phi_i^2 \tau \tag{23}$$

where

$$\tau = \frac{4a^2 t}{L^2}$$

Let $\tau = \tau^*$ be the time at which the strain reaches its peak value, $\varepsilon = \varepsilon_{max}$. Then the generalized strain $\bar{\varepsilon}$ may be expressed as

$$\bar{\varepsilon} = 2 \sum_{i=1}^{\infty} \frac{1}{\phi_i} \frac{\tan \phi_i + \tanh \phi_i}{\dfrac{1}{\cos^2 \phi_i} - \dfrac{1}{\cosh^2 \phi_i} + \dfrac{2M}{\phi_i^2}} \sin \phi_i^2 \tau^* \tag{24}$$

12

Since the eigenvalues ϕ_i are functions of M only, and since τ^* is a dimensionless quantity chosen to maximize a function of M, it can be seen that $\bar{\varepsilon}$ is a function of M only, or

$$\bar{\varepsilon} = \bar{\varepsilon}(M)$$

5. McQuillen Solution

The sensitivity of the infinite series in ε, Eq. (23), to small changes in t, makes it difficult to find the maximum value of the strain. To facilitate this, McQuillen et al. [5] have modified the Clebsch solution by distributing the impactor mass and non-vanishing initial velocity of the beam over a small distance d on either side of the center of the beam. Mathematically, the mass distribution is

$$\bar{Q}(x) = \frac{m_1}{L} + \frac{m_2}{2d} \{ H[x - (\frac{L}{2} - d)\,]$$

$$- H[x - (\frac{L}{2} + d)]\}$$

where H is the unit step function. The initial conditions are then

$$w(x,0) = 0$$

$$\frac{\partial w}{\partial t}(x,0) = v_0\{H[x - (\frac{L}{2} - d)] - H[x - (\frac{L}{2} + d)]\}$$

where

$$v_0 = \frac{v}{\frac{2dM}{L} + 1} \cdot$$

The solution is assumed to have the same vibration mode shapes as the original concentrated-mass system, and the coefficients of a truncated series are evaluated using Galerkin's method. The new solution in strain is better behaved with respect to time, so that evaluating the approximate maximum by a search method is more convenient.

13

In Fig. 5, the results of this solution are presented for a fixed value of d/L (= 0.02667). Note that in this solution $\bar{\epsilon}$ is also a function of M only, and all impact cases are represented by a single curve.

6. Timoshenko Solution

As can be seen from Table I, the most sophisticated model to be considered is the Timoshenko solution, which uses continuous mass distribution and includes the contact force [6]. The static Hertz's law of contact, Eq. 12, is assumed between the beam and impactor

$$F = k_2 \, \alpha^{3/2}$$

The displacement of the midspan point of a simply supported beam due to a dynamic force F applied at midspan, using the Euler-Bernoulli equation, is

$$w_1 = \frac{2L}{\rho A \pi^2 a^2} \sum_{i=1,3,5}^{\infty} \frac{1}{i^2} \int_0^t F(\tau) \, \sin \frac{i^2 \pi^2 a^2}{L^2} (t-\tau) d\tau \qquad (25)$$

Using Newton's law, the displacement of the impactor may be written as

$$w_2 = vt - \frac{1}{m_2} \int_0^t \int_0^t F \, dt \, dt \qquad (26)$$

The last three quations may be combined into a single nonlinear integral equation in terms of the contact force F

14

$$\left[\frac{F}{k_2}\right]^{2/3} = vt - \frac{1}{m_2}\int_0^t\int_0^t F\,dt\,dt$$

(27)

$$- \frac{2L}{\rho A \pi^2 a^2} \sum_{i=1,3,5}^{\infty} \frac{1}{i^2} \int_0^t F(\tau) \sin\frac{i^2\pi^2 a^2}{L^2}(t-\tau)d\tau$$

which may be solved numerically by the small-increment method, as described in Appendix B.

A typical calculated contact-force history is presented in Fig. 6, showing the phenomenon of multiple sub-impacts. The contact-force predicted by the two-degrees-of-freedom mass-spring model for the same problem is included for comparison.

Due to the nonlinearity of Eq. (12), the beam deflection and strain are functions of at least three parameters, M, k_2, and v, or

$$\bar\varepsilon = \bar\varepsilon(M,k_2,v)\ .$$

Thus, a two-parameter family of $\bar\varepsilon$ vs. M curves must be constructed to represent all impact situations. It can be shown, however, that the dependence of $\bar\varepsilon$ on k_2 and v is weak, so that a single curve gives a good approximation of all impact cases. In order to demonstrate this, a parametric calculation was made, with different values of the following parameters: flexural rigidity EI, contact stiffness k_2, and impact velocity v. The actual values used, as well as the calculated values of $\bar\varepsilon$, are all summarized in Table II. The same results are also plotted in Fig. 5 as a shaded strip to indicate the slight spread of data in the $\bar\varepsilon$ vs. M plane.

15

An inspection of Table II and Fig. 5 indicates that, for any value of M, the maximum change in $\bar{\epsilon}$ due to doubling other parameters is only 11%. In particular, the largest change in $\bar{\epsilon}$ due to a 100% change in impact velocity alone is only 4%. Since by Eq. (5), $\epsilon_{max} \propto v \bar{\epsilon}$, it may be concluded that the maximum strain is very nearly linearly proportional to the impact velocity.

The effect of internal damping in the beam has been included in the Timoshenko solution by Hoppmann [7]. We have made calculations with similar damping included and found no appreciable change in deflection or strain for the range of impact problems considered (low mass ratio M).

The effect of local plastic deformation at the impact point has also been considered [8]. The use of a plastic, rather than Hertzian, contact law, however, had only a small effect on the maximum bending strain. Both internal damping and the plastic contact law as applied to the Timoshenko solution are discussed in detail in Appendix B.

III. Experiments

A series of experiments was conducted to compare with the theoretical calculations. Beams of various dimensions and materials were impacted at midspan by blunt (25.4-mm contact radius) cylindrical steel impactors fired from a 25.4-mm bore-diameter compressed-air gun. The beams were supported by rounded (3.2-mm radius) blade supports positioned as close as practical to each end opposite the air gun. Four types of beam specimens were used: (1) flat aluminum beams, 200 mm span, 2.31 mm depth, and three widths, 76.5 mm, 40 mm, and 30 mm; (2) an aluminum beam, 152 mm span, 20 mm width, and 12.7 mm depth; (3) a steel beam, 98 mm span, 15.1 mm width, and 9.0 mm

16

depth; (4) a graphite-epoxy laminated beam, 96.5 mm span, 38.1 mm width, and 1.6 mm depth. The graphite-epoxy specimens were fabricated from 0.132 mm-thick Hercules AS3501 prepreg tape at a lay-up of $(\pm 45/0_2/\mp 45)_S$. Bending strain was monitored by a 1/8-in (3.2-mm) strain gage (Micro-Measurements, Inc., types EA-06-125AD-120 and EA-13-125AD-120) mounted on the beam directly opposite the impact point, and recorded on a Tektronix Type 565 oscilloscope. The impact velocity was determined by recording two stroboscopic exposures of the impactor just before impact, measuring the distance between the images, and timing the interval between exposures using the oscilloscope and a photodiode system. The relative error in the velocity measurement is estimated at $\pm$ 1% and in the strain measurement at $\pm$ 3%.

Another series of experiments was conducted using a drop-weight apparatus to impact the steel beam described above, and another steel beam, 197 mm span, 15.9 mm width and depth. Impact velocity was determined from the drop height in this case.

Figure 7 shows two of the measured strains as functions of time. These two strain curves were recorded on the same beam impacted by the same projectile at two different velocities. As can be seen from the figure, the general shapes of the curves are similar, and the magnitudes are proportional to the impact velocity.

The results of our experiments, as well as of a few experiments conducted by others [9,10], are summarized in Table III. They are also plotted in Fig. 8 in the $\bar{\epsilon}$ vs. M plane. These results will be discussed in the next section.

Also conducted were a series of impact-to-failure experiments on graphite-epoxy beams of various sizes and lay-ups. These are discussed in detail in Appendix C.

17

The flexural rigidity EI of each type of graphite-epoxy beam specimen used in the impact experiments was determined by a static three-point bending test. In each test the load and deflection were measured and the flexural rigidity was calculated from the static beam flexure formula. The flexural rigidity was also calculated from laminated-plate theory by assuming that $EI = D_x b$, and approximately the same value was obtained in each case.

18

IV. Discussion and Design Application

1. Comparison of Results

Among the six analytical solutions, the four that neglect the contact force all yield relations of the form $\bar{\epsilon} = \bar{\epsilon}(M)$; that is, the generalized strain is a function of M only. The other two solutions show that $\bar{\epsilon}$ depends weakly on other parameters. In Fig. 5, the $\bar{\epsilon}$ vs. M curves from the two one-degree-of-freedom models and the McQuillen solution are all distinct curves. The curve from the Timoshenko solution is shown as a narrow strip indicating the spread of values of $\bar{\epsilon}$ due to changes in other parameters. The spread in $\bar{\epsilon}$ calculated by the two-degrees-of-freedom model due to variation of the stiffness ratio $K = K_1/K_2$ is so small, however, that these results are plotted as a simple line. The Clebsch solution is not shown in Fig. 5.

The Timoshenko solution has lower values of $\bar{\epsilon}$ as compared with the McQuillen solution. In the former, the impactor may rebound, retaining part of the total energy, whereas in the latter, the impactor retains no kinetic energy when the maximum deflection and strain are reached. If the Clebsch solution were shown, it should be slightly higher than McQuillen's because Clebsch's conserves the total energy; McQuillen's solution balances the momentum of the impactor and a small portion of the beam, thus losing part of the initial kinetic energy. The portion of the beam that acquires initial velocity is small, thus the loss of energy is also very small.

The same discussion can be applied to the lumped-mass models. The energy-conserved model gives the highest strain, and the momentum-conserved model gives the lowest strain.

19

It can also be seen from Fig. 5 that the continuous-mass models give higher strain than the lumped-mass models. This may be attributed to the fact that in the higher modes of beam vibration, which are not considered by the simpler models, more bending strain is produced per unit of strain energy.

The experimentally measured strain is in general lower than the calculated value. In Fig. 9, the measured and calculated strains at the back surface of the beam at midspan are compared. The general shapes of the curves are in agreement. The peak strain calculated by the Timoshenko solution is approximately 36% higher than the measured one. This discrepancy could be due to a combination of material damping, plastic effects, inaccuracy in material properties, and inaccuracy in strain measurement.

It is interesting to note that within each solution method, or following one series of experiments, a single $\bar{\varepsilon}$ vs. M curve can be constructed to represent approximately all impact situations. This result implies that for values of M less than about two, the most important parameter in structural response is the mass ratio M; the contact stress has direct influence on the details of the multiple sub-impacts, but has little effect on the maximum strain. It is also demonstrated that the strain is directly proportional to the impact velocity.

2. Design Applications

Additional research is needed to ascertain the reasons for the discrepancy between the analytical models and the experiments. None of the analytical models can be used with certainty to precisely predict strain.

20

The present results, however, are already useful to designers in predicting trends and approximate values.

The designer may use the present curves of the one-degree-of-freedom models for beam impact problems. He may choose the Timoshenko model, and add whatever necessary refinements, such as plastic contact stress and material damping, and obtain a new $\bar{\epsilon}$ vs. M curve. He may also choose to conduct a series of experiments at low impact speeds, each experiment at a different value of M. The resulting $\bar{\epsilon}$ vs. M curve can then be used for predicting the strain due to higher-speed impacts.

To use the design curve in Figs. 5 or 8, compute first the beam-to-impactor mass ratio M, then locate the corresponding value of $\bar{\epsilon}$ from the curve. The maximum bending strain can then be found from Eq. (5). If failure of the structure is assumed to be associated with the maximum strain, then an impact-to-failure experiment may be conducted and the calculated maximum strain for this impact condition can be considered as the ultimate dynamic strain.

The present paper has concentrated on transverse impact of simply supported beams, but the same procedure can be easily applied to other types of structures. In general, a separate $\bar{\epsilon}$ vs. M curve must be constructed for each given _type_ of structure. For instance, the problem of central impact of clamped and simply supported orthotropic plates is currently being solved by the same method and will be presented in a separate report.

The analytical methods discussed here can be used for impact problems with any value of M. The design curve, $\bar{\epsilon}$ vs. M, however, is a single curve only in the region of small values of M, M < 2. For larger values of M (smaller impactor mass), some other dimensionless parameters must be developed to represent the impact. This is currently being pursued.

21

V.   List of Symbols

a^2 = $\sqrt{EI/\rho A}$

b = width of beam

EI = flexural rigidity of beam

F = contact force

h = depth of beam

k_2 = Hertzian contact stiffness

K_1 = equivalent beam spring constant

K_2 = linearized contact stiffness (spring constant)

$K = K_1/K_2$ = stiffness ratio

L = length of beam

m_1 = mass of beam

m_2 = mass of impactor

m_e = $(17/35)m_1$ = effective mass of beam

M = m_1/m_2

t = time

v = velocity of impactor before impact

v_0 = initial velocity immediately after impact

w = $w(x,t)$ = beam deflection

(= $w(x)$ = static beam deflection)

w_1 = $w_1(t)$ = deflection of beam at midspan

(= deflection of equivalent beam mass)

(= static deflection at midspan)

$w_{1_{max}}$ = maximum midspan deflection

w_2 = $w_2(t)$ = displacement of impactor

x = beam axial coordinate

z = distance from beam neutral axis

α = contact approach = $w_2 - w_1$

δ = static midspan deflection of beam

22

$$\varepsilon \quad = \quad \varepsilon(t) = \text{bending strain at midspan}$$

$$\varepsilon_{max} \quad = \quad \text{maximum value of } \varepsilon(t)$$

$$\bar{\varepsilon} \quad = \quad \text{generalized strain} = \varepsilon_{max} \, a^2/hv$$

$$\rho A \quad = \quad \text{linear density of beam}$$

$$\tau \quad = \quad \text{dimensionless time} = 4ta^2/L^2$$

$$\phi_i \quad = \quad \text{eigenvalues}$$

$$\cdot \quad = \quad \text{time derivative}$$

VI. References

1. Goldsmith, W., <u>Impact, the Theory and Physical Behavior of Colliding Solids</u>, Edward Arnold, Ltd., London, 1960.

2. Young, T., "Natural Philosophy," J. Johnson, London, 1807, Vol. 1, p. 147, Vol. 2, p. 50.

3. Cox, H., "On Impact of Elastic Beams," Transactions of the Cambridge Philosophical Society, Vol. 9, 1856, part 1, p. 73.

4. Clebsch, A., Théorie de ℓ'élasticité des corps solides, translated by A. J. St.-Venant and A. Flamant. Paris, Dunod, 1883.

5. McQuillen, E.J., Llorens, R.E., and Gause, L.W. "Low Velocity Transverse Normal Impact of Graphite Epoxy Composite Laminates," Report No. NADC-75119-30, Naval Air Development Center, Warminster, Pa., June, 1975.

6. Timoshenko, S.P., "Zur Frage nach der Wirkung eines Stosses auf einen Balken," Z. Math. Phys., Vol. 62 (1913) No. 2, pp. 198-209.

7. Hoppmann, W.H., "Impact of a Mass on a Damped Elastically Supported Beam," Trans. ASME, Journal of Applied Mechanics, Vol. 70, 1948, p. 125.

8. Crook, A.W., "A Study of Some Impacts Between Metal Bodies by a Piezo-electric Method," Proc. Royal Soc. London, A212, 1952, p. 377.

9. Jelinek, J.J., "Impact of a Mass on a Beam," Thesis (M.S.), Univ. of Calif., Berkeley, 1943.

10. Arnold, R.N., "Impact Stresses in a Freely Supported Beam," Proceedings of Institution of Mechanical Engineers, Vol. 137, 1937, p. 217.

11. Barnhart, K.E., Jr., and Goldsmith, W., "Stresses in Beams During Transverse Impact," J. Appl. Mech., Trans. ASME, Vol. 79, 1957, p. 440.

24

Table I. Summary of Simplified Models for the Beam Impact Problem.

	Contact Force Neglected		Contact Force Included
	Energy Conserved	Momentum Conserved	
Lumped Mass	One-degree-of-freedom (Young)	One-degree-of-freedom (Cox)	Two-degree-of-freedom
Continuous Mass	Clebsch	McQuillen	Timoshenko

25

Table II. Impact cases calculated by the Timoshenko solution.

(impact velocity, v_0 = 6.1 m/sec; contact stiffness constant,
$k_{2,0}$ = 2.27 x 10^{11} N/$m^{3/2}$; beam flexural rigidity, EI_0 = 3.533 N-m^2)

M	v/v_0	$k_2/k_{2,0}$	EI/EI_0	$\bar{\epsilon}$
0.01	1	1	1	9.006
	2	1	1	8.933
	1	2	1	8.921
	1	1	2	9.036
0.05	1	1	1	4.241
	2	1	1	4.233
	1	2	1	4.284
	1	1	2	4.218
0.1	1	1	1	3.122
	2	1	1	2.996
	1	2	1	3.236
	1	1	2	3.429
0.5	1	1	1	1.766
	2	1	1	1.660
	1	2	1	1.737
	1	1	2	1.574

Table III. Beam Impact Experiments

Beam material and dimension, L x b x h (mm)	Impactor mass, m_2(kg)	Mass ratio, $M=m_1/m_2$	Impact velocity, v(m/sec)	Maximum strain, $\epsilon \times 10^6$	Generalized strain, $\bar{\epsilon}$
Steel 102x15.1x9.0 (drop weight)	.816	0.1315	2.44	3100	1.895
	.816	0.1315	3.44	4600	1.990
	1.043	0.1029	2.44	3650	2.231
	1.043	0.1029	3.44	5300	2.293
	1.724	0.0622	2.44	4200	2.567
Steel 102x15.1x9.0 (air gun)	.0567	1.893	3.90	1200	0.458
	.0567	1.893	6.40	2000	0.465
	.110	0.978	3.44	1550	0.670
	.110	0.978	5.82	2600	0.665
Aluminum 152x20x12.7 (air gun)	.0567	1.93	4.39	1500	0.475
	.0567	1.93	6.92	2300	0.462
	.110	0.998	3.96	1900	0.667
	.110	0.998	6.19	3050	0.686
Aluminum 203x76.2x2.3 (air gun)	.110	0.908	3.11	2300	0.892
	.110	0.908	6.34	4380	0.997
Aluminum 203x40x2.3 (air gun)	.0567	0.923	2.90	1650	0.822
	.0567	0.923	7.01	3900	0.803
	.110	0.477	3.05	2700	1.278
	.110	0.477	6.74	5100	1.092
Aluminum 203x30x2.3 (air gun)	.0567	0.692	2.87	1810	0.912
	.0567	0.692	7.07	4300	0.877
	.110	0.357	3.32	3300	1.433
	.110	0.357	6.80	5980	1.269
Steel [9] 775x25.4x25.4 (drop weight)	1.819	2.16	.408	143	0.506
	1.819	2.16	1.27	483	0.548
	1.819	2.16	1.78	700	0.568
	4.314	0.909	.381	278	1.053
	4.314	0.909	.762	672	1.271
	4.314	0.909	1.01	983	1.396

Table III (continued)

Beam material and dimensions L x b x h (mm)	Impactor mass, m_2 (kg)	Mass ratio, $M=m_1/m_2$	Impact velocity v(m/sec)	Maximum strain, $\varepsilon_{max} \times 10^6$	Generalized strain, $\bar{\varepsilon}=\varepsilon_{max}\dfrac{a^2}{hv}$
Steel, Ref. [10] (8-ft section of 112-1b/yd railway rail) (drop weight)	44.5	3.05	3.46	680	0.45
	108.6	1.25	3.46	1300	0.86
	213.6	0.635	3.46	1720	1.14
Graphite-epoxy Composite, AS3501, 96.5x38.1x1.6 (air gun)	0.0144	0.599	4.75	2400	0.776
	0.0144	0.599	9.88	5400	0.840
	0.0144	0.599	13.08	6200	0.728
	0.0281	0.307	4.72	4100	1.336
	0.0281	0.307	6.08	5000	1.263
	0.0281	0.307	7.04	5100	1.113
	0.0568	0.152	4.33	4500	1.595
	0.0568	0.152	6.72	7500	1.714
	0.110	0.0785	3.36	5400	2.47
	0.110	0.0785	3.97	5900	2.28
	0.110	0.0785	7.56	11200	2.28
Steel, 197x15.9x15.9 (drop weight)	0.795	0.487	2.44	1840	1.120
	0.795	0.487	3.46	2400	1.033
	1.05	0.368	2.44	2125	1.294
	1.05	0.368	3.46	3100	1.334
	1.73	0.223	2.44	2575	1.568
	1.73	0.223	3.46	3800	1.635

(a) before impact   (b) at maximum deflection
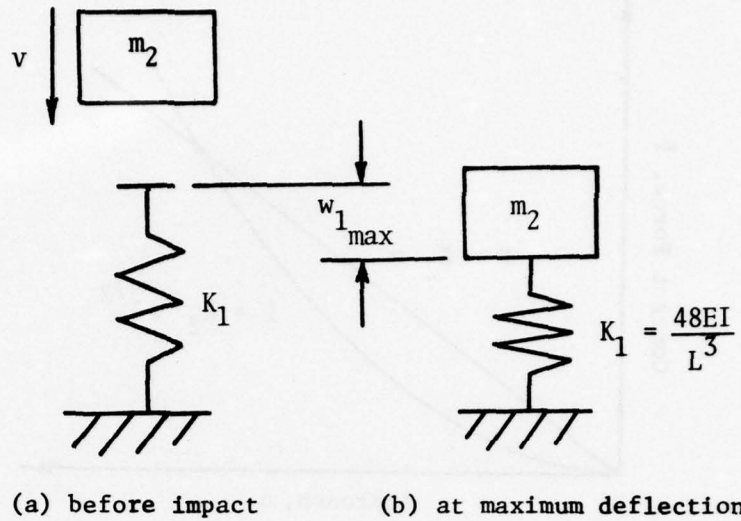
Figure 1. One-degree-of-freedom model of beam impact, conservation of energy.

(a) before impact   (b) immediately after impact
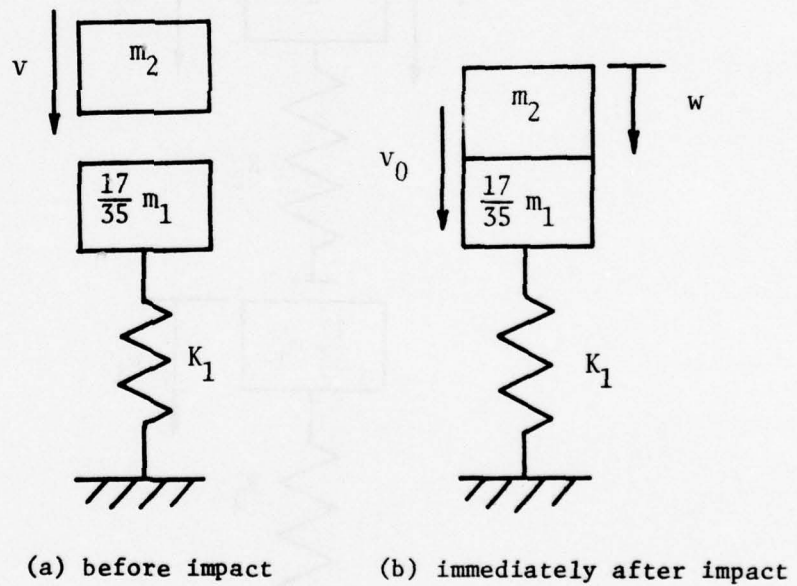
Figure 2. One-degree-of-freedom (Cox) model of beam impact, conservation of momentum.
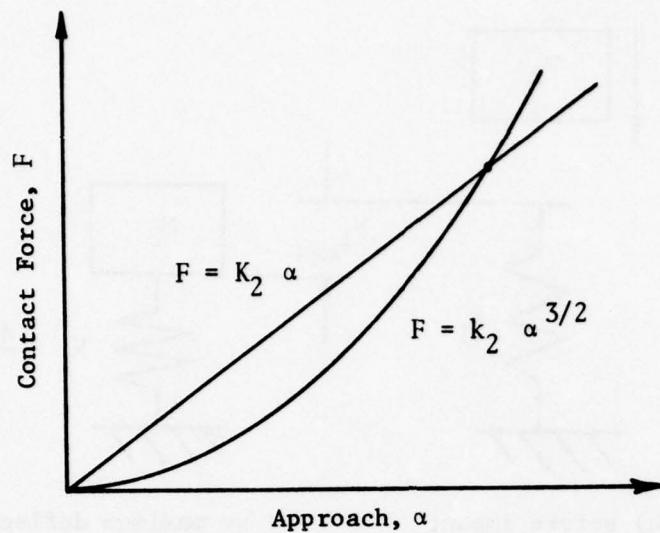
Figure 3. Linear approximation of Hertzian contact stiffness.
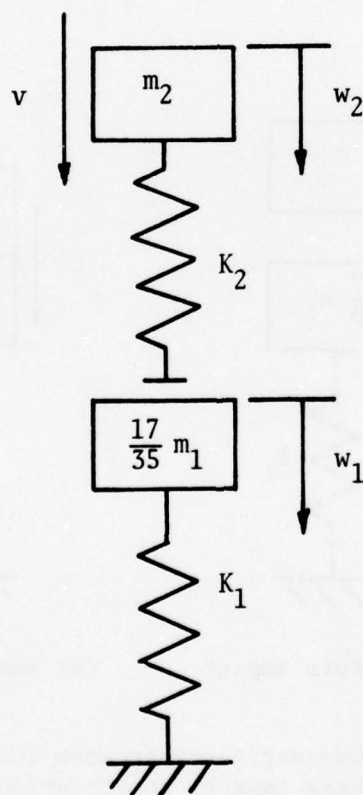
Figure 4. Two-degrees-of-freedom model of beam impact.

30
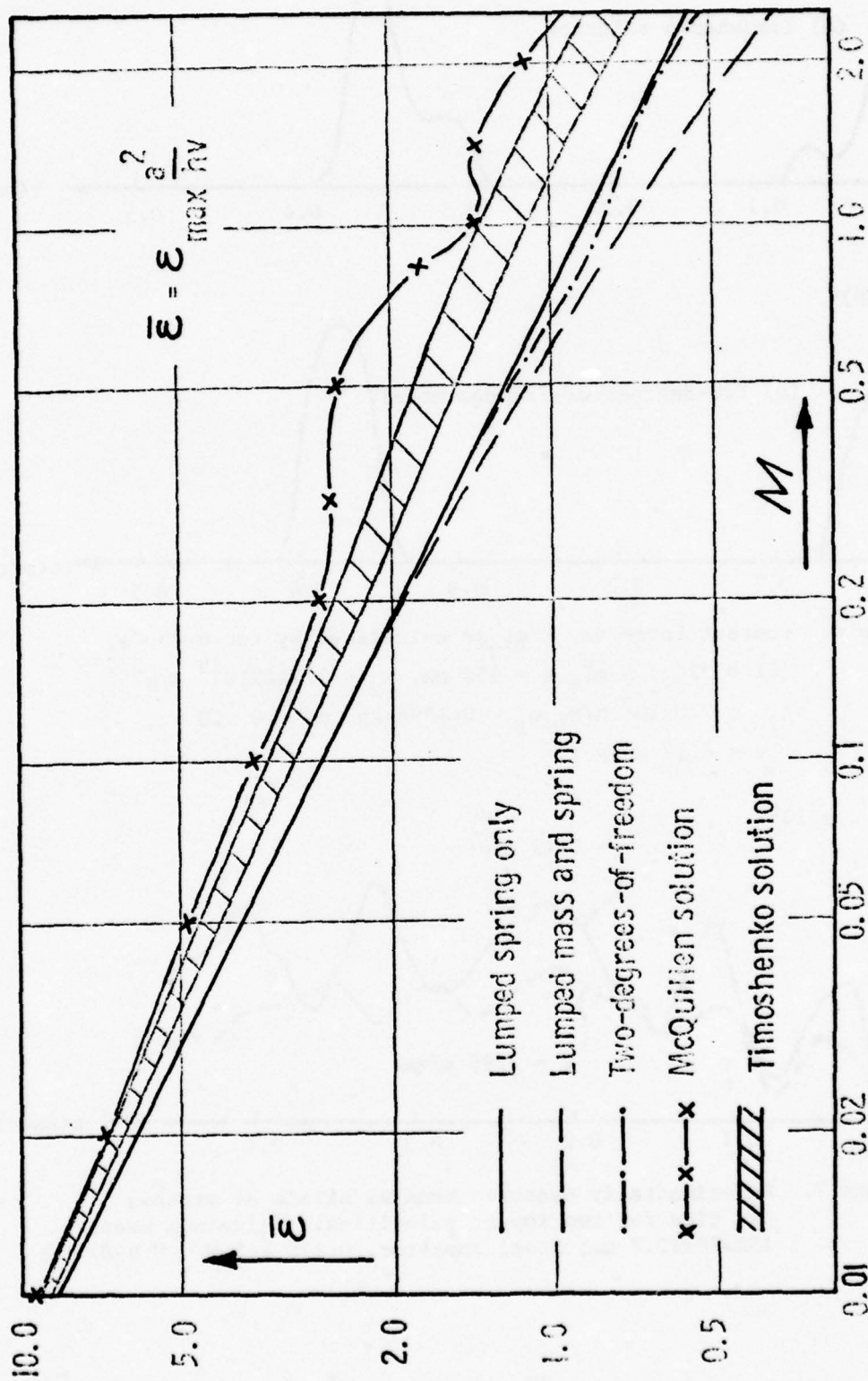
Figure 5. Generalized strain $\bar{\varepsilon}$ vs. mass ratio M curves as calculated by five different methods for simply supported beams subjected to central impact.

$$\bar{\varepsilon} = \varepsilon_{max} \frac{a^2}{hv}$$

Lumped spring only

Lumped mass and spring

Two-degrees-of-freedom

McQuillen solution

Timoshenko solution

F(KN)

10

5

0

(a) Timoshenko solution

t(msec)

0   0.1   0.2   0.3   0.4   0.5

F(KN)

10

5

0

(b) Two-degrees-of-freedom model

t(msec)

0   0.1   0.2   0.3   0.4   0.5
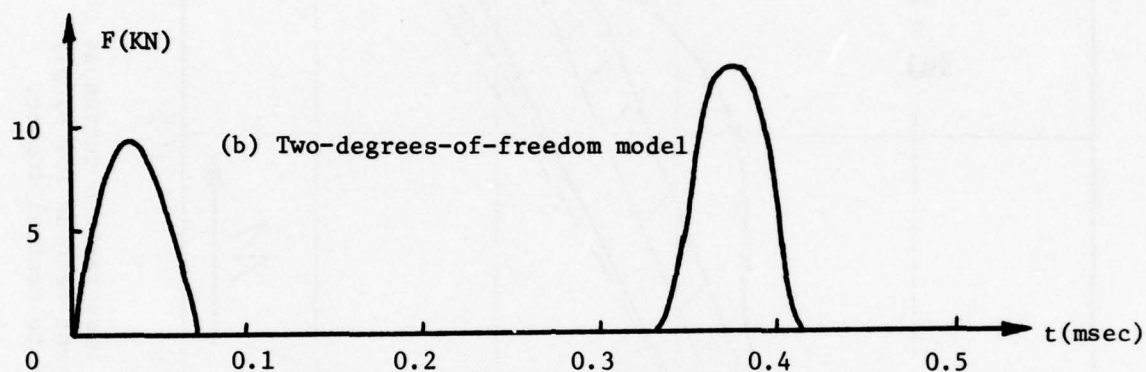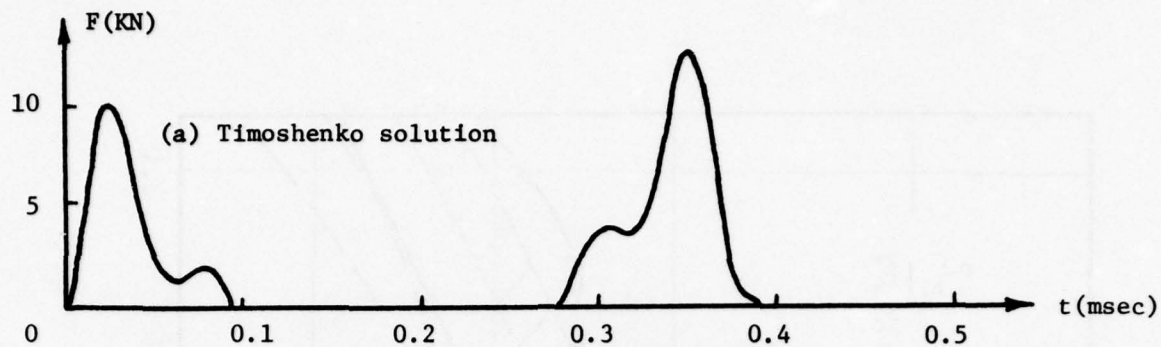
Figure 6. Contact force vs. time as calculated by two methods.
(EI = 224.1 N-m^2, L = 152 mm, k$_2$ = 1.744x10^{19} N/m$^{3/2}$
K$_2$ = 7.0x10^7 N/m, m$_1$ = 0.1096 kg, m$_2$ = 0.110 kg,
v = 6.19 m/sec).

ε x 10^6

v = 6.19 m/sec

3000

2000

1000

v = 3.96 m/sec

t(msec)

0   0.1   0.2   0.3   0.4
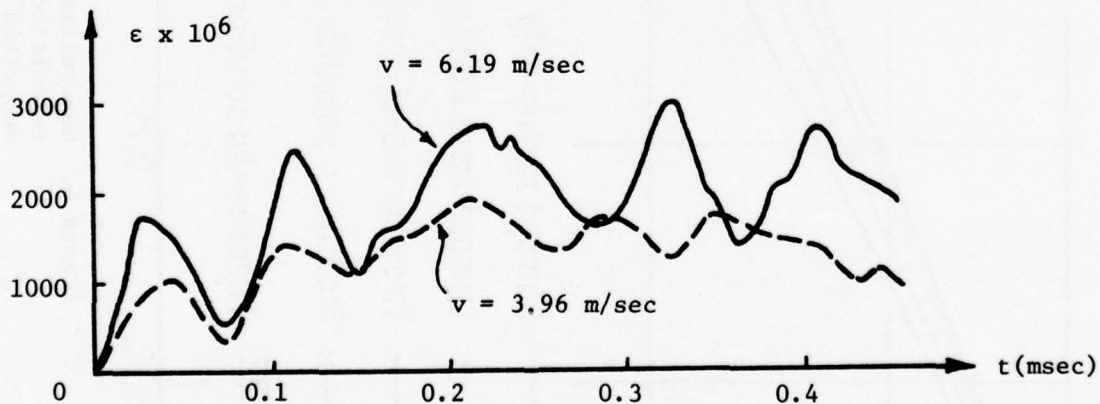
Figure 7. Experimentally measured bending strain at midspan
vs. time for two impact velocities. (Aluminum beam,
152x20x12.7 mm; steel impactor, 0.110 kg; M = 0.998)

32
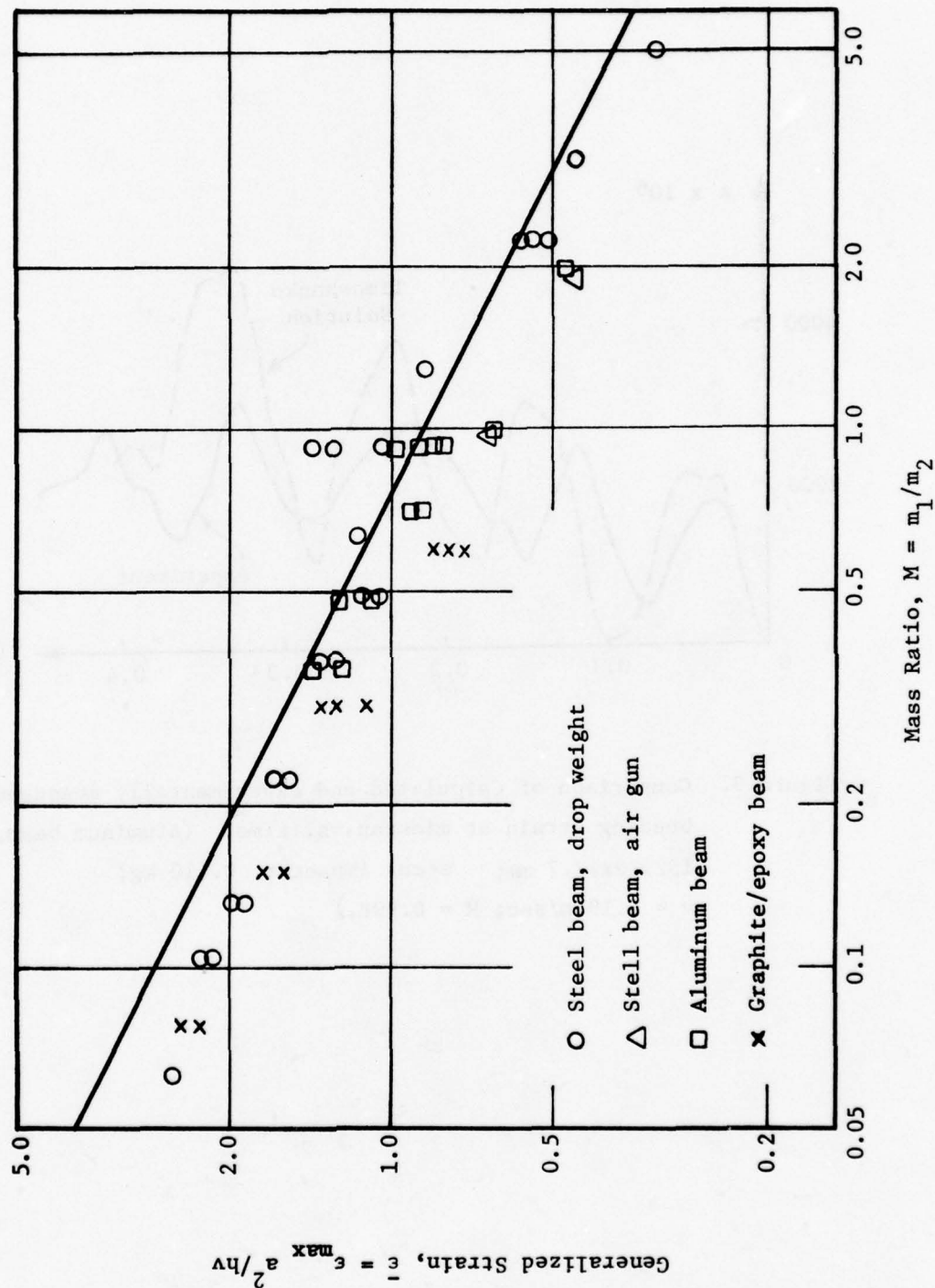
Figure 8. Experimental Impact Data and One Possible Design Curve.

33
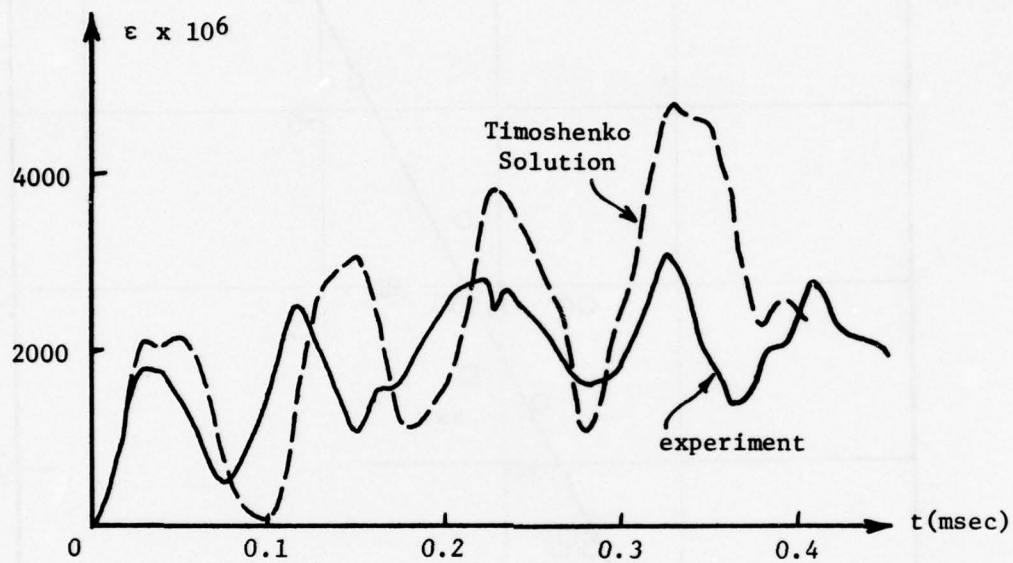
Figure 9. Comparison of Calculated and experimentally measured
bending strain at midspan vs. time. (Aluminum beam,
152x20x12.7 mm; steel impactor, 0.110 kg;
v = 6.19 m/sec; M = 0.998.)

34

Appendix A - Two-Degrees-of-Freedom Model of Beam Impact

Presented in this appendix are the details of the solution for the motion of the two-degrees-of-freedom model of beam impact depicted in Fig. 4. Equations (15) and (16), which govern the motion of this system, are repeated here for convenience, substituting the symbol m_e for the effective mass of the beam, $(17/35)m_1$.

$$\left.\begin{aligned} m_e\ddot{w}_1 + K_2(w_1 - w_2) + K_1 w_1 &= 0 \\ m_2\ddot{w}_2 + K_2(w_2 - w_1) &= 0 \end{aligned}\right\} \quad \begin{aligned} &\text{if } w_1 \le w_2 \\ &\text{(in contact)} \end{aligned} \tag{A1}$$

$$\left.\begin{aligned} \ddot{w}_2 &= 0 \\ m_e\ddot{w}_1 + K_1 w_1 &= 0 \end{aligned}\right\} \quad \begin{aligned} &\text{if } w_1 > w_2 \\ &\text{(during separation)} \end{aligned}$$

We shall first solve the former pair of equations, which govern the motion of the system when the spring K_2 is compressed, i.e., when the impactor is in contact with the beam. The natural frequencies of this system are

$$\omega^2 = \frac{m_e K_2 + m_2(K_1 + K_2) \pm \{[m_e K_2 + m_2(K_1 + K_2)]^2 - 4m_e m_2 K_1 K_2\}^{\frac{1}{2}}}{2m_e m_2} \tag{A2}$$

The solution for the displacements due to free vibration in terms of the initial displacements and velocities is

$$\begin{aligned} w_1(\tau) &= AC_1 \sin(\omega_1 \tau + \phi_1) + BC_2 \sin(\omega_2 \tau + \phi_2) \\ w_2(\tau) &= A \sin(\omega_1 \tau + \phi_1) + B \sin(\omega_2 \tau + \phi_2) \end{aligned} \tag{A3}$$

where

$$\phi_1 = \tan^{-1}\left[\frac{w_1(0) - w_2(0)C_2}{\dot{w}_1(0) - \dot{w}_2(0)C_2}\,\omega_1\right]$$

$$\phi_2 = \tan^{-1}\left[\frac{w_1(0) - w_2(0)C_1}{\dot{w}_1(0) - \dot{w}_2(0)C_1}\,\omega_2\right]$$

$$A = \frac{\dot{w}_1(0) - \dot{w}_2(0)C_2}{\omega_1(C_1 - C_2)\cos\phi_1}$$

35

$$B = \frac{\dot{w}_1(0) - \dot{w}_2(0)C_1}{\omega_2(C_2 - C_1) \cos \phi_2}$$

$$C_i = 1 - \omega_i^2 \frac{m_2}{K_2}$$

and $\tau = t - t_0$ is the time relative to the instant $t = t_0$ for which the initial displacements and velocities are know.

During separation, the latter pair of equations in system (A1) describes the motion of a simple one-degree-of-freedom mass-spring system (m_e, K_1) in free vibration and of the impactor mass m_2 in free flight. The solution of the equations is

$$w_1(\tau) = \frac{\dot{w}_1(0)}{\Omega} \sin \Omega\tau + w_1(0) \cos \Omega\tau$$

$$w_2(\tau) = w_2(0) + \tau \dot{w}_2(0)$$

(A4)

where $\Omega = [K_1/m_e]^{\frac{1}{2}}$

The calculation of Eqs. (A3) and (A4) is accomplished with the aid of the computer according to the following procedure

1. The initial conditions

$$w_1(0) = w_2(0) = 0$$

$$\dot{w}_1(0) = 0$$

$$\dot{w}_2(0) = v$$

where v is the impact velocity, are substituted into Eqs. (A3). These equations are solved for the displacements at small intervals of time. The strain in the beam may be derived from the displacement w_2 through Eq. 4. If and when w_1 becomes larger than w_2, separation occurs and the final values of $w_1, w_2, \dot{w}_1$, and $\dot{w}_2$ are saved for the next step of the procedure.

36

2. The saved values of the displacements and velocities are substituted as initial conditions into Eqs. (A4). These equations are also solved at small intervals of time, until w_2 becomes greater than w_1, i.e., a second collision takes place. The values of $w_1, w_2, \dot{w}_1$, and $\dot{w}_2$ are again stored.

3. For the second collision the stored values are used as initial conditions for Eqs. (A3), which are solved until separation again occurs.

4. The solution then alternates between Eqs. (A3) and Eqs. (A4) according to the relative values of w_1 and w_2, i.e., depending on whether beam and impactor are separated or in contact.

For large values of the mass ratio M (greater than about 1.0), only one collision takes place. For smaller values of M, several collisions may occur, as the impactor mass m_2 follows the beam mass m_e as it deflects.

A listing and sample output of the FORTRAN computer program used to calculate the equations are included at the end of this appendix. The sample problem treated has the following parameters.

$$m_1 = 0.1 \text{ kg}$$
$$m_2 = 1.0 \text{ kg}$$
$$K_1 = 2.0 \times 10^6 \text{ N/m}$$
$$K_2 = 20.0 \times 10^6 \text{ N/m}$$
$$v = 2.0 \text{ m/sec}$$
$$L = 0.20 \text{ m}$$
$$h = 0.01 \text{ m}$$

Displacements, velocities and contact force are calculated at 0.1 μsec intervals and printed out every tenth interval.

37

It is interesting to consider a dimensionless form of Eqs. (A1).
Defining the quantities

$$K = K_1/K_2 \qquad\qquad M = m_1/m_2$$

$$\omega = (K_1/m_1)^{\frac{1}{2}} \qquad\qquad \bar{\tau} = \omega\tau/\sqrt{K}$$

$$y_1 = \omega\, w_1/v \qquad\qquad y_2 = \omega\, w_2/v$$

then Eqs. (A1) may be written as

$$\left.\begin{aligned} \frac{d^2y_1}{d\bar{\tau}^2} + (K + 1)\, y_1 + y_2 &= 0 \\[2mm] \frac{d^2y_2}{d\bar{\tau}^2} + \frac{17}{35} M(y_2 - y_1) &= 0 \end{aligned}\right\} \quad \text{if } y_1 \le y_2$$

$$\left.\begin{aligned} \frac{d^2y_2}{d\bar{\tau}^2} &= 0 \\[2mm] \frac{17}{35}\,\frac{d^2y_1}{d\bar{\tau}^2} + y_1 &= 0 \end{aligned}\right\} \quad \text{if } y_1 > y_2$$

Observation of these equations indicates that, for small values of
the parameter K (K<<1), the response in terms of maximum deflection y_1 or
w_1 of the beam is not significantly dependent on the value of K. Further,
the peak bending strain ε_{max}, which is assumed proportional to the maximum
deflection (Eq. (4)) is also relatively independent of K. Therefore, M
is the only significant parameter in determining the response of the beam
to impact, for small values of K. This is in agreement with our numerical
calculation and experimental results discussed earlier. In most actual
beam-impact problems, the appropriate value of K is quite small, since the
resistance of the beam to local indentation K_2 is much larger than its
deflection stiffness K_1.

38

```fortran
C         TWODOF -- COMPUTER PROGRAM FOR SOLVING TWO-DEGREE-OF-FREEDOM
C                   MODEL OF BEAM IMPACT
C             K1 - BEAM BENDING STIFFNESS
C             M1 - BEAM EFFECTIVE MASS
C             MB - ACTUAL BEAM MASS
C             K2 - HERTZ CONTACT STIFFNESS
C             M2 - IMPACTOR MASS
C             V  - IMPACT VELOCITY
C*************************************************************************
      REAL M1,M2,K1,K2,K,M,L,MB
      COMMON Y1,Y2,V1,V2,OMEGA1,OMEGA2,OMEGAN,Y11,Y12,Y21,Y22,C,D,PHI1,
     1 PHI2
      PI=3.14159265
  200 FORMAT(5X,"TIME",13X,"Y1",12X,"Y2",13X,"V1",13X,"V2",10X,"APPROACH
     1",7X,"REL. VEL.",7X,"FORCE",6X,"STRAIN")
C     INPUT DATA
      V=2.0
      MB=0.1
      M2=1.0
      K1=2.0E06
      K2=20.0E06
      L=0.2
      H=0.01
C         INITIAL CONDITIONS
      Y10=0.
      Y20=0.
      V10=0.
      V20=V
      K=K1/K2
      M=MB/M2
      M1=17.0*MB/35.0
   40 FORMAT(30X,"K =",E15.8,30X,"M =",E15.8,/)
C     CALCULATE NATURAL FREQUENCIES
      OMEGAN=SQRT(K1/M1)
      TERM1=M1*K2+M2*(K1+K2)
      TERM2=TERM1**2-4.0*M1*M2*K1*K2
      TERM2=SQRT(TERM2)
      OMEGA1=(TERM1+TERM2)/(2.0*M1*M2)
      OMEGA2=(TERM1-TERM2)/(2.0*M1*M2)
      OMEGA1=SQRT(OMEGA1)
      OMEGA2=SQRT(OMEGA2)
      OMEGAH=SQRT(K2/M2)
      C=1.0-OMEGA1**2/OMEGAH**2
      D=1.0-OMEGA2**2/OMEGAH**2
C         SET UP TIME SCALE
      TFINAL=1.2E-03
      DT=0.1E-06
      N=TFINAL/DT
      NSKIP=10
      IFLAG=0
C     COMPUTE DISPLACEMENTS AND VELOCITIES
      DO300I=0,N
      T=I*DT
      IF(T.GT.(DT/2.))GOTO1
      CALLCONTACT(T,TZERO,Y10,Y20,V10,V20,IFLAG)
      ALPHA=Y2-Y1
      RELVEL=V2-V1
      IF(IFLAG.EQ.0)STOP
```

```
        GOTO301
      1 ALPHA=Y2-Y1
        IF(ALPHA.LT.0.)GOTO3
        CALLCONTACT(T,TZERO,Y10,Y20,V10,V20,IFLAG)
        ALPHA=Y2-Y1
        RELVEL=V2-V1
        IF(MOD(I,NSKIP).NE.0)GOTO300
        GOTO301
      3 CALL APART (T,TZERO,Y10,Y20,V10,V20,IFLAG,MULTIM)
        ALPHA=Y2-Y1
        RELVEL=V2-V1
        IF(MOD(I,NSKIP).NE.0)GOTO300
    100 FORMAT(1X,E12.5,8(2X,E13.6))
    301 CONTINUE
        EX=6.0*B*Y1/L**2
        F=K2*ALPHA
        IF(MOD((I/NSKIP),59).NE.0)GOTO302
 COLUMN HEADINGS
        PRINT 201
    201 FORMAT(1H1)
        PRINT 200
    302 PRINT 100,T,Y1,Y2,V1,V2,ALPHA,RELVEL,F,EX
    300 CONTINUE
        PRINT40,K,M
        STOP
        END
```

```
      SUBROUTINE APART (T,TZERO,Y10,Y20,V10,V20,IFLAG,MULTIM)
      COMMON Y1,Y2,V1,V2,P1,P2,OMEGAN,Y11,Y12,Y21,Y22,C,U,PHI1,PHI2
      SN=SIN(OMEGAN*(T-TZERO))
      CN=COS(OMEGAN*(T-TZERO))
      Y1=V10*SN/OMEGAN+Y10*CN
      V1=V10*CN-Y10*OMEGAN*SN
      Y2=Y20+V20*(T-TZERO)
      V2=V20
      IFLAG=1
      ALPHA=Y2-Y1
CHECK WHETHER BEAM AND IMPACTOR HAVE RE-COLLIDED
      IF(ALPHA.LT.0.)RETURN
      IFLAG=0
      MULTIM=MULTIM+1
      TZERO=T
      Y10=Y1
      Y20=Y2
      V10=V1
      V20=V2
      RETURN
      END
```

41

```
      SUBROUTINECONTACT(T,TZERO,Y10,Y20,V10,V20,IFLAG)
      COMMON X1,Y2,V1,V2,P1,P2,OMEGAN,Y11,Y12,Y21,Y22,C,D,PHI1,PHI2
      IF(IFLAG.EQ.1)GOTO1
      TERM1=Y10-Y20*C
      TERM2=(V10-V20*C)/P2
      PHI2=ATAN2(TERM1,TERM2)
      Y22=TERM2/(D-C)/COS(PHI2)
    3 TERM1=Y10-Y20*D
      TERM2=(V10-V20*D)/P1
      PHI1=ATAN2(TERM1,TERM2)
      Y21=TERM2/(C-D)/COS(PHI1)
   13 Y11=Y21*C
      Y12=Y22*D
    1 S1=SIN(P1*(T-TZERO)+PHI1)
      S2=SIN(P2*(T-TZERO)+PHI2)
      Y1=Y11*S1+Y12*S2
      Y2=Y21*S1+Y22*S2
      C1=P1*COS(P1*(T-TZERO)+PHI1)
      C2=P2*COS(P2*(T-TZERO)+PHI2)
      V1=Y11*C1+Y12*C2
      V2=Y21*C1+Y22*C2
      IFLAG=1
      ALPHA=Y2-Y1
CHECK WHETHER BEAM AND IMPACTOR HAVE SEPARATED
      IF(ALPHA.GE.0.)RETURN
      IFLAG=0
      TZERO=T
      Y10=Y1
      Y20=Y2
      V10=V1
      V20=V2
      RETURN
      END
```

42

```
    TIME          Y1            Y2            V1            V2           APPROACH      REL. VEL.      FORCE         STRAIN
 .0            .0            .0            .0            .200000E 01   .0            .200000E 01   .0            .0
 .10000E-05    .137252E-09   .199999E-05   .411748E-03   .199998E 01   .199986E-05   .199957E 01   .399971E 02   .205877E-09
 .20000E-05    .109794E-08   .399995E-05   .164650E-02   .199992E 01   .399885E-05   .199827E 01   .799770E 02   .164690E-08
 .30000E-05    .370509E-08   .599982E-05   .370457E-02   .199982E 01   .599611E-05   .199612E 01   .119922E 03   .555764E-08
 .40000E-05    .878099E-08   .799957E-05   .658408E-02   .199968E 01   .799079E-05   .199310E 01   .159816E 03   .131715E-07
 .50000E-05    .171467E-07   .999917E-05   .102840E-01   .199950E 01   .998202E-05   .198922E 01   .199640E 03   .257201E-07
 .60000E-05    .296218E-07   .119986E-04   .148025E-01   .199928E 01   .119659E-04   .198448E 01   .239379E 03   .444327E-07
 .70000E-05    .470239E-07   .139977E-04   .201375E-01   .199902E 01   .139507E-04   .197888E 01   .279014E 03   .705359E-07
 .80000E-05    .701682E-07   .159965E-04   .262865E-01   .199872E 01   .159264E-04   .197244E 01   .318528E 03   .105252E-06
 .90000E-05    .998673E-07   .179951E-04   .332466E-01   .199838E 01   .178953E-04   .196514E 01   .357906E 03   .149801E-06
 .10000E-04    .136931E-06   .199933E-04   .410144E-01   .199801E 01   .198564E-04   .195699E 01   .397128E 03   .205396E-06
 .11000E-04    .182164E-06   .219911E-04   .495864E-01   .199759E 01   .218090E-04   .194800E 01   .436180E 03   .273246E-06
 .12000E-04    .236370E-06   .239885E-04   .589584E-01   .199713E 01   .237521E-04   .193818E 01   .475043E 03   .354555E-06
 .13000E-04    .300346E-06   .259854E-04   .691260E-01   .199664E 01   .256851E-04   .192751E 01   .513701E 03   .450519E-06
 .14000E-04    .374686E-06   .279815E-04   .800844E-01   .199611E 01   .276069E-04   .191602E 01   .552138E 03   .562329E-06
 .15000E-04    .460777E-06   .299776E-04   .918284E-01   .199554E 01   .295168E-04   .190371E 01   .590337E 03   .691165E-06
 .16000E-04    .558802E-06   .319728E-04   .104352E 00   .199493E 01   .314140E-04   .189057E 01   .628281E 03   .838204E-06
 .17000E-04    .669740E-06   .339675E-04   .117651E 00   .199428E 01   .332977E-04   .187663E 01   .665954E 03   .100461E-05
 .18000E-04    .794360E-06   .359614E-04   .131717E 00   .199360E 01   .351670E-04   .186188E 01   .703341E 03   .119154E-05
 .19000E-04    .933427E-06   .379546E-04   .146544E 00   .199287E 01   .370212E-04   .184633E 01   .740424E 03   .140014E-05
 .20000E-04    .108770E-05   .399471E-04   .162126E 00   .199211E 01   .388594E-04   .182999E 01   .777189E 03   .163155E-05
 .21000E-04    .125793E-05   .419388E-04   .178454E 00   .199132E 01   .406809E-04   .181287E 01   .813618E 03   .188669E-05
 .22000E-04    .144485E-05   .439298E-04   .195521E 00   .199049E 01   .424849E-04   .179497E 01   .849698E 03   .216720E-05
 .23000E-04    .164921E-05   .459198E-04   .213320E 00   .198962E 01   .442706E-04   .177630E 01   .885412E 03   .247382E-05
 .24000E-04    .187173E-05   .479090E-04   .231841E 00   .198872E 01   .460372E-04   .175686E 01   .920745E 03   .280760E-05
 .25000E-04    .211313E-05   .498972E-04   .251076E 00   .198778E 01   .477841E-04   .173670E 01   .955682E 03   .316970E-05
 .26000E-04    .237412E-05   .518845E-04   .271015E 00   .198681E 01   .495104E-04   .171579E 01   .990208E 03   .356110E-05
 .27000E-04    .265540E-05   .538708E-04   .291650E 00   .198580E 01   .512154E-04   .169415E 01   .102431E 04   .398309E-05
 .28000E-04    .295765E-05   .558561E-04   .312971E 00   .198476E 01   .528985E-04   .167179E 01   .105797E 04   .443647E-05
 .29000E-04    .328156E-05   .578403E-04   .334967E 00   .198368E 01   .545588E-04   .164872E 01   .109118E 04   .492234E-05
 .30000E-04    .362780E-05   .598235E-04   .357628E 00   .198257E 01   .561957E-04   .162495E 01   .112391E 04   .544171E-05
 .31000E-04    .399704E-05   .618055E-04   .380943E 00   .198143E 01   .578084E-04   .160049E 01   .115617E 04   .599555E-05
 .32000E-04    .438990E-05   .637863E-04   .404902E 00   .198026E 01   .593964E-04   .157536E 01   .118793E 04   .658486E-05
 .33000E-04    .480705E-05   .657660E-04   .429492E 00   .197906E 01   .609589E-04   .154957E 01   .121918E 04   .721057E-05
 .34000E-04    .524910E-05   .677444E-04   .454703E 00   .197782E 01   .624953E-04   .152312E 01   .124991E 04   .787364E-05
 .35000E-04    .571665E-05   .697216E-04   .480523E 00   .197656E 01   .640050E-04   .149604E 01   .128010E 04   .857499E-05
 .36000E-04    .621034E-05   .716975E-04   .506938E 00   .197526E 01   .654872E-04   .146833E 01   .130974E 04   .931551E-05
 .37000E-04    .673073E-05   .736721E-04   .533938E 00   .197394E 01   .669414E-04   .144000E 01   .133883E 04   .100961E-04
 .38000E-04    .727841E-05   .756454E-04   .561508E 00   .197259E 01   .683670E-04   .141108E 01   .136734E 04   .109176E-04
 .39000E-04    .785393E-05   .776173E-04   .589636E 00   .197121E 01   .697634E-04   .138157E 01   .139527E 04   .117809E-04
 .40000E-04    .845786E-05   .795878E-04   .618309E 00   .196980E 01   .711299E-04   .135149E 01   .142260E 04   .126860E-04
 .41000E-04    .909073E-05   .815509E-04   .647513E 00   .196836E 01   .724662E-04   .132085E 01   .144932E 04   .136361E-04
 .42000E-04    .975306E-05   .835245E-04   .677234E 00   .196690E 01   .737715E-04   .128966E 01   .147543E 04   .146296E-04
 .43000E-04    .104454E-04   .854907E-04   .707458E 00   .196541E 01   .750453E-04   .125795E 01   .150091E 04   .156680E-04
 .44000E-04    .111681E-04   .874553E-04   .738171E 00   .196390E 01   .762872E-04   .122573E 01   .152574E 04   .167522E-04
 .45000E-04    .119219E-04   .89418[illegible]-04   .769358E 00   .196236E 01   .774966E-04   .119300E 01   .154993E 04   .178826E-04
 .46000E-04    .127070E-04   .91380[illegible]-04   .801005E 00   .196080E 01   .786730E-04   .115979E 01   .157346E 04   .190605E-04
 .47000E-04    .135240E-04   .93340[illegible]-04   .833096E 00   .195921E 01   .798160E-04   .112612E 01   .159632E 04   .202860E-04
 .48000E-04    .143733E-04   .95298[illegible]-04   .865617E 00   .195760E 01   .809251E-04   .109199E 01   .161850E 04   .215600E-04
 .49000E-04    .152554E-04   .97255[illegible]-04   .898551E 00   .195598E 01   .819999E-04   .105742E 01   .164000E 04   .228831E-04
 .50000E-04    .161706E-04   .992104E-04   .931884E 00   .195432E 01   .830398E-04   .102244E 01   .166080E 04   .242559E-04
 .51000E-04    .171193E-04   .101104E-03   .965600E 00   .195265E 01   .840446E-04   .987034E 00   .168089E 04   .256789E-04
 .52000E-04    .181019E-04   .103116E-03   .999682E 00   .195096E 01   .850138E-04   .951281E 00   .170026E 04   .271526E-04
 .53000E-04    .191188E-04   .105066E-03   .103412E 01   .194925E 01   .859470E-04   .915138E 00   .171894E 04   .286782E-04
 .54000E-04    .201702E-04   .107014E-03   .106888E 01   .194753E 01   .868440E-04   .878043E 00   .173688E 04   .302554E-04
 .55000E-04    .212566E-04   .108961E-03   .110397E 01   .194578E 01   .877042E-04   .841013E 00   .175408E 04   .318850E-04
 .56000E-04    .223783E-04   .110906E-03   .113935E 01   .194402E 01   .885275E-04   .804064E 00   .177055E 04   .335674E-04
 .57000E-04    .235354E-04   .112849E-03   .117502E 01   .194224E 01   .893134E-04   .767215E 00   .178627E 04   .353032E-04
 .58000E-04    .247264E-04   .114790E-03   .121096E 01   .194045E 01   .900618E-04   .729484E 00   .180124E 04   .370926E-04
```

Appendix B.   Timoshenko Solution - Numerical Scheme, Damping and
                Plastic Contact Effects

In this appendix, the details of the solution of Timoshenko's equation
for beam impact, Eq. (27), are presented. Also included are discussions
of the application of internal damping effects and a plastic contact law
to the Timoshenko method, as well as a procedure for averaging the computed
strain over a small distance for more exact comparison with strain measured
during impact experiments using a strain gage.

Numerical Scheme

Eq. (27), which is repeated here for convenience,

$$\alpha = \left[\frac{F}{k_2}\right]^{2/3} = vt - \frac{1}{m_2} \int_0^t \int_0^t F \, dt \, dt$$

$$- \frac{2L}{\rho A \pi^2 a^2} \sum_{i=1,3,5}^{\infty} \frac{1}{i^2} \int_0^t F(\tau) \sin \frac{i^2 \pi^2 a^2}{L^2} (t-\tau) \, d\tau \qquad (27)$$

may be numerically solved by applying the small-increment method in which
the contact force F is assumed to be constant during any time increment $\Delta\tau$.
Expanding the above integrals to compute the force during the nth time
interval F_n, we obtain the following.

$$\left(\frac{F_n}{k_2}\right)^{2/3} = vn\Delta\tau - \frac{(\Delta\tau)^2}{m_2} \sum_{j=1}^{n} D_{n-j+1} F_j$$

$$- \frac{2L^3}{\pi^4 EI} \sum_{j=1}^{n} E_{n-j+1} F_j \qquad (B1)$$

where

$$E_{n-j+1} = \sum_{i=1,3,5}^{\infty} \frac{1}{i^4} \left[\cos \frac{i^2 \pi^2 a^2}{L^2} (n-j)\Delta\tau - \cos \frac{i^2 \pi^2 a^2}{L^2} (n-j+1)\Delta\tau\right] \quad (B2)$$

44

If the contact force is approximated as a linear continuous function of time, with an average value of F_j during the jth time step, then

$$\sum_{j=1}^{n} D_{n-j+1} F_j = 2[(n-1)F_1 + (n-2)(F_2 - F_1) +$$

$$(n-3)(F_3 - F_2 + F_1) + \cdots + (n-j)(F_j - F_{j-1} + F_{j-2} - \cdots \pm F_1)$$

$$+ \cdots + (F_{n-1} - F_{n-2} + F_{n-3} - \cdots \pm F_1)]$$

$$+ \frac{1}{3}(F_n - F_{n-1} + F_{n-2} - \cdots \mp F_1)$$

(B3)

Computer calculation of numbers raised to fractional powers involves the use of the logarithm and antilogarithm functions, each of which requires the machine-time-consuming evaluation of a truncated series. For the sake of computer efficiency, Eq. (B1) was first rewritten as a cubic equation in F_n so that all terms are raised to integral powers only. The resulting equation is solved for each successive time increment by means of Newton's iterative method.

Having found the contact-force history, one may determine the maximum beam deflection and maximum bending strain, both of which occur at midspan.

$$w(L/2, t) = \frac{2L^3}{EI \pi^4} \sum_{j=1}^{n} E_{n-j+1} F_j$$

(B4)

$$\varepsilon(L/2, t) = \frac{hL}{EI \pi^2} \sum_{j=1}^{n} H_{n-j+1} F_j$$

(B5)

45

where

$$H_{n-j+1} = \sum_{i=1,3,5}^{\infty} \frac{1}{i^2} \left[\cos \frac{i^2\pi^2 a^2}{L^2} (n-j)\Delta\tau - \cos \frac{i^2\pi^2 a^2}{L^2} (n-j+1)\Delta\tau \right]$$

Note that the bending-strain coefficients H_{n-j+1} converge much more slowly than the deflection coefficients E_{n-j+1}.

Strain Averaging

In the beam impact experiments, strain in the beam was measured using resistance-wire strain gages. These devices measure strain not at a point, but over a finite, though small, area. In order to make a more rigorous comparison between experimental results and theoretical calculations, the computed strain may be averaged over a distance corresponding to the length of the strain gage.

The strain due to bending for any point on the beam may be expressed as

$$\varepsilon(x,t) = \sum_{i=1,3,5}^{\infty} A_i(t)(-1)^{\frac{i-1}{2}} \sin \frac{i\pi x}{L} \tag{B6}$$

where

$$A_i(t) = \frac{h}{m_1 a^2} \int_0^t F(\tau) \sin \frac{i^2\pi^2 a^2}{L^2} (t-\tau)d\tau$$

Let ε_{avg} be the average strain within a distance δ on either side of the impact point $x = L/2$. Then

$$\varepsilon_{avg}(t) = \frac{1}{2\delta} \int_{L/2-\delta}^{L/2+\delta} \varepsilon(x,t)dx \tag{B7}$$

Substitution and integration leads to

46

$$\varepsilon_{avg}(t) = \sum_{i=1,3,5}^{\infty} A_i(t) \frac{\sin \frac{i\pi\delta}{L}}{\frac{i\pi\delta}{L}} \tag{B8}$$

The average strain may thus be calculated from the contact-force history determined by the small-increment solution using the following equation

$$\varepsilon_{avg}(t) = \frac{hL}{EI\,\pi^2} \sum_{j=1}^{n} \bar{H}_{n-j+1} F_j \tag{B9}$$

where

$$\bar{H}_{n-j+1} = \sum_{i=1,3,5}^{\infty} \frac{1}{i^2} \left[\cos \frac{i^2\pi^2 a^2}{L^2}(n-j)\Delta\tau - \cos \frac{i^2\pi^2 a^2}{L^2}(n-j+1)\Delta\tau \right] \frac{\sin \frac{i\pi\delta}{L}}{\frac{i\pi\delta}{L}}$$

For the typical case of a 1/8-inch (3.175 mm) strain gage attached to a beam of span 96.5 mm, $\delta/L = 0.01645$. The following corresponding values may be computed for the averaging factor.

i	1	5	11	15	31
$\dfrac{\sin \frac{i\pi\delta}{L}}{\frac{i\pi\delta}{L}}$	0.9996	0.9889	0.9470	0.9028	0.6239

It may be seen from the table and Eq. (B8) that the effect of averaging the strain is to diminish the contributions of the higher modes of beam vibration. For cases where the impactor is massive compared to the beam (low mass ratio M), however, the beam response is largely restricted to the lowest several modes of vibration. Thus, averaging the strain for the cases studied made little difference in the value of the strain at any given time (less than 1% decrease)

47

Internal Damping

Hoppmann [7] has extended the Timoshenko solution of beam impact to include the effects of internal and external damping and elastic foundation. If internal damping only is considered, the equation for the contact force corresponding to Eq. (27) is

$$\alpha = \left[\frac{F}{k_2}\right]^{2/3} = vt - \frac{1}{m_2} \int_0^t \int_0^t F \, dt \, dt$$

$$- \frac{2}{\rho AL} \sum_{i=1,3,5}^{\infty} \frac{1}{\theta_i} \int_0^t F(\tau) \sin \theta_i(t-\tau) e^{-\delta_i(t-\tau)} d\tau \tag{B10}$$

where

$$\theta_i = \sqrt{p_i^2 - \delta_i^2}$$

$$p_i = \pi^2 i^2 a^2 / L^2$$

$$\delta_i = \frac{\pi^4 i^4}{L^4} \frac{c_1 I}{2\rho A}$$

where c_1 is the internal damping coefficient.

Application of the small-increment integration method to this equation yields the following equation in F_n, the force during the nth time interval.

$$\left[\frac{F_n}{k_2}\right]^{2/3} = vn\Delta\tau - \frac{(\Delta\tau)^2}{m_2} \sum_{j=1}^{n} D_{n-j+1} F_j$$

$$- \frac{2L^3}{\pi^4 EI} \sum_{j=1}^{n} E^*_{n-j+1} F_j \tag{B11}$$

48

where

$$E^*_{n-j+1} = \sum_{i=1,3,5}^{\mu} \frac{1}{i^4} \left\{ \exp[-\delta_i(n-j)\Delta\tau] \right.$$

$$\left[\frac{\delta_i}{\theta_i} \sin \theta_i(n-j)\Delta\tau + \cos \theta_i(n-j)\Delta\tau\right]$$

$$\left. - \exp[-\delta_i(n-j+1)\Delta\tau] \left[\frac{\delta_i}{\theta_i} \sin \theta_i(n-j+1)\Delta\tau + \cos \theta_i(n-j+1)\Delta\tau\right] \right\}$$

where μ is the number of the highest underdamped mode. Note that when damping is absent, $\delta_i = 0$ and the above system reduces to Eqs. (B1) and (B2). The last term in Eq. (B11) is also the expression for the deflection at midspan.

The expression for the bending strain at midspan is

$$\varepsilon(L/2, t) = \frac{hL}{\pi^2 EI} \sum_{j=1}^{n} H^*_{n-j+1} F_j \tag{B12}$$

where

$$H^*_{n-j+1} = \sum_{i=1,3,5}^{\mu} \frac{1}{i^2} \left\{ \exp[-\delta_i(n-j)\Delta\tau] \right.$$

$$\left[\frac{\delta_i}{\theta_i} \sin \theta_i(n-j)\Delta\tau + \cos \theta_i(n-j)\Delta\tau\right]$$

$$\left. - \exp[-\delta_i(n-j+1)\Delta\tau] \cdot \left[\frac{\delta_i}{\theta_i} \sin \theta_i(n-j+1)\Delta\tau + \cos \theta_i(n-j+1)\Delta\tau\right] \right\}$$

49

Overdamped modes were not considered for two reasons. First, the lowest overdamped mode is quite high for a moderate amount of damping. In a numerical example, Hoppmann uses a value of the fractional damping factor $\beta_n = \delta_n/p_n$ for the fundamental mode of $\beta_1 = 0.002$; for this case, the lowest overdamped mode is n = 23. Even for $\beta_1 = 0.008$, the lowest overdamped mode is n = 13. For low values of beam-to-impactor mass ratio M, these higher modes are not significantly excited. Second, overdamped modes are nonoscillatory, and, once excited, contribute to the response of the system for only a short period of time.

Figure (B1) illustrates the effect of a rather large amount of internal damping on the bending strain calculated by the Timoshenko solution. Note that the general shape of both curves (damped and undamped) is quite similar, indicating that the first mode of beam vibration is not significantly affected by damping. The smaller oscillations due to the higher modes, however, are noticeably attenuated after several cycles.

Plastic Contact Law

The above formulations of the Timoshenko solution are based on Hertz's law of contact

$$F = k_2 \, \alpha^{3/2}$$

a static relation which treats the two bodies as elastic. As suggested by Crook [8] and Barnhart and Goldsmith [11], a contact law may also be used which treats the beam and impactor as behaving plastically at the impact point.

The following assumptions are made:

1. The initial elastic behavior before the onset of yielding is neglected.

2. The normal stress, or flow pressure, is constant over the area of contact during plastic indentation.

3. The plastic flow of the material in the contact zone is not considered.

4. Restitution of the plastically deformed region is elastic.

These assumptions lead to a force-indentation law which may be written as

$$F = \bar{k}_2 \, \alpha \qquad \text{for } \dot{\alpha} > 0, \text{ (approaching phase)} \qquad \text{(B13)}$$

$$F = F_m \left[\frac{\alpha - \alpha_r}{\alpha_m - \alpha_r} \right]^{3/2} \qquad \text{for } \dot{\alpha} < 0, \text{ (rebound phase)} \qquad \text{(B14)}$$

where $\bar{k}_2 = 2\pi R \, p_0$, R is the radius of the impactor, p_0 is the dynamic flow pressure of the beam, F_m and α_m are the values of the contact force and indentation at the instant of maximum penetration, and α_r is the depth of the permanent crater. Defining the recovery ratio $\eta = \alpha_r / \alpha_m$, then the latter relation may be written as

$$F = \frac{F_m}{\alpha_m} \left[\frac{\frac{\alpha}{\alpha_m} - \eta}{1 - \eta} \right]^{3/2}$$

51

The contact law thus described is represented in Fig. (B2). In the beam impact problems studied, multiple sub-impacts occur; therefore, repeated indentations must be considered. For simplicity, the permanent crater created by one sub-impact was neglected in the next sub-impact. However, if during the elastic recovery in a particular sub-impact the contact force again increases, plastic deformation is assumed to begin again (Fig. B3).

This contact law may be substituted for Eq. (12) in the Timoshenko solution and the response of a beam to plastic impact may be calculated. Choosing values for the recovery ratio $\alpha_r/\alpha_m = 0.5$ and the plastic stiffness constant $k_2 = 2.0 \times 10^5$ lb/in, the solution of a typical problem using the plastic contact law was compared with a solution using the Hertzian elastic law (Fig. B4). Note that the shapes of the two curves are quite similar but that the effect of the plastic contact law is to reduce the maximum bending strain.

Computer Programs

Listings and sample outputs of the FORTRAN computer programs used to calculate the response of the beam according to the above methods are presented in the following pages.

The first listing presents the program SMINC1, which includes the calculations for strain averaging and the effects of internal damping.

52

The values of the parameters of the sample problem are:

$$m_1 = 0.1 \text{ kg}$$

$$m_2 = 0.1 \text{ kg}$$

$$E = 2.1 \times 10^{11} \text{ N/m}^2$$

$$L = 0.20 \text{ m}$$

$$b = 0.012 \text{ m}$$

$$h = 0.012 \text{ m}$$

$$k_2 = 2.4 \times 10^{11} \text{ N/m}^{3/2}$$

$$v = 6.0 \text{ m/sec}$$

$$\delta = 0.002 \text{ m} \quad \text{(strain-averaging distance)}$$

$$\beta_1 = 0.02 \quad \text{(damping ratio)}$$

The contact force is calculated at 1.0-μsec intervals and substituted into Eqs. (B4) and (B5) (or Eqs. (B9) and (B12) if strain averaging and damping are included) to obtain the deflection and strain at midspan.

The second listing presents SMINC2, which includes the effect of plastic deformation at the impact point. The same problem as described above is again treated, with the additional parameters,

$$\eta = 0.5$$

$$\bar{k}_2 = 1.0 \times 10^{10} \text{ N/m} \quad .$$

```
C        SMINC1 -- DAMPING INCLUDED, STRAIN AVERAGING
C
COMPUTATION OF TIMOSHENKO"S SMALL INCREMENT SOLUTION OF HERTZIAN IMPACT
C                       OF A SIMPLE BEAM
C        DT - TIME INCREMENT
C        NDT - NO. OF TIME INCREMENTS CALCULATED
C        NH - NO. OF BEAM MODES CONSIDERED
C        TOL - TOLERANCE OF ERROR IN NONLINEAR SOLUTION
C        PR1, PR2 - POISSON"S RATIO OF BEAM, IMPACTOR
C        V - IMPACT VELOCITY
C        R1 - RADIUS OF IMPACTOR
C        FI - FLEXURAL RIGIDITY
C        H, B, L - THICKNESS, WIDTH, SPAN OF BEAM
C        RHO1, RHO2 - DENSITY OF BEAM, IMPACTOR
C        K2 - HERTZIAN CONTACT STIFFNESS
C        M1, M2 - MASS OF BEAM, IMPACTOR
C        DELTA - HALF-WIDTH OF STRAIN GAGE
         REAL L,M1,M2,K2,M
         DIMENSION F(4500),G(4500),Z(4500),E(4500)
C     ABOVE DIMENSIONS MUST BE GREATER THAN NDT
  1001 FORMAT(4X,"N",10X,"T",16X,"F(N)",16X,"ALPHA",12X,"STRAIN",9X,
      1 "AVER. STRAIN",6X,"NONDIM. STRAIN",5X,"DEFLECTION")
C     INPUT DATA
         NH=40
         NDT=50
         TOL=1.0E-05
         BETA1=0.002
         V=6.0
         M1=0.1
         M2=1.0
         FI=2.1E 11
         L=0.20
         H=0.012
         B=0.012
         FI=2.1E 11
         K2=2.4E11
         DELTA =0.0016
         DT=0.1E-06
C*****************************************************************************
         PI=3.14159265398
         M=M1/M2
         FI=E1*H**3*B/12
         A2=SQRT(EI*L/M1)
         Q=1./3.
         S=2./3.
         PRINT 1002,DT,A2,M,K2,DELTA,FI
  1002 FORMAT("   DT = ",F13.6,"   A**2 = ",F13.6,"   M = ",E13.6,"   K2 =
      1",F13.6,"     DELTA =",F13.6,"     EI =",E13.6)
         PRINT1001
         B=DT**2/3.0/M2
         DO90K=1,NDT
         Z(K)=0
         F(K)=0.
   90    G(K)=0
C     IF NO DAMPING, USE SIMPLER CALCULATIONS
         IF(BETA1.EQ.0.0)GOTO91
         C=2.0/M2
         CC=PI**2*H/2./L**2*C
```

54

```
                OMEGA1=PI**2*A2/L**2
                DELTA1=BETA1*OMEGA1
                IF(DELTA1.NE.0.)GOTO30
                ICRIT=NH
                GOTO31
C        FIND CRITICALLY DAMPED MODE
        30 ICRIT=SQRT(OMEGA1/DELTA1)
                IF(MOD(ICRIT,2).EQ.0)ICRIT=ICRIT-1
                IF(ICRIT.GT.NH)ICRIT=NH
CONSIDER UNDERDAMPED MODES ONLY
        31 DO6I=1,ICRIT,2
                J=I**2
                JJ=J**2
                C2=1.0
                TERM3=I*PI*DELTA/L
                FTA=SIN(TERM3)/TERM3
                DELTAI=DELTA1*JJ
                OMEGAI=OMEGA1*J
                THETAI=SQRT(OMEGAI**2-DELTAI**2)
                RATIO=DELTAI/THETAI
                DO6K=1,NDT
                T=K*DT
                C1=C2
                C2=EXP(-DELTAI*T)*(COS(THETAI*T)+RATIO*SIN(THETAI*T))
                TERM=(C1-C2)/OMEGAI**2
                Z(K)=Z(K)+TERM*J
                F(K)=F(K)+TERM*J*FTA
         6 G(K)=G(K)+TERM
                GOTO32
        91 C=2.0*L**3/(EI*PI**4)
                CC=L*H/EI/PI**2
                TERM1=PI**2*A2*DT/L**2
                DO16I=1,NH,2
                J=I**2
                TERM2=J*TERM1
                JJ=J**2
                C2=1.0
                TERM3=I*PI*DELTA/L
                FTA=SIN(TERM3)/TERM3
                DO 16 K=1,NDT
                C1=C2
                C2=COS(K*TERM2)
                TERM=C1-C2
CREATE TABLE OF SUMMATION FUNCTIONS
                Z(K)=Z(K)+TERM/J
                F(K)=F(K)+TERM/J*FTA
        16   G(K)=G(K)+TERM/JJ
        32 P=B+C*G(1)
COLUMN HEADINGS
                DO100N=1,NDT
                IF(MOD(N,60).NE.0)GOTO70
      1003 FORMAT(1H1)
                PRINT1003
                PRINT1001
C              DETERMINE THE FORCE F
        70 T=N*DT
                A=V*T
                IF(N.EQ.1)GOTO14
```

55

```
       RUM=0.
       NM1=N-1
       SUMI=0.
       SUM=0.
       DO5J=1,NM1
       K=N-J
       R=K
       SUMI=F(J)-SUMI
       SUM=SUM+R*SUMI
    5  RUM=RUM+F(J)*G(K+1)
       A=A-C*RUM
       A=A-DT**2*(2.*SUM-SUMI/3.)/M2
C               ITERATIVE SOLUTION FOR F(N) USING NEWTON"S METHOD
       FNEW=FNEW+TOL
       GOTO13
   14  FNEW=A/(P+2./3./K2)
       FNEW=FNEW/100.
   13  FN=FNEW
       B=SIGN(1.0,FN)/K2**2-3.0*A*P**2
       FFN=P**3*FN**3+B*FN**2
    I      +3.0*A**2*P*FN-A**3
       FPFN=3.0*P**3*FN**2+2.0*B*FN+3.0*A**2*P
   82  FNEW=FN-FFN/FPFN
       ERROR=ABS((FNEW-FN)/FN)
       IF(ERROR.GT.TOL)GOTO13
       IF(N.GT.1)GOTO10
       IF(FNEW.GT.0.)GOTO10
       FNEW=-FNEW
       GOTO13
   10  F(N)=FNEW
       IF(FNEW.LT.0.)F(N)=0.
CALCULATE STRAIN AND DEFLECTION
       EPS=0.
       EPSTAR=0.
       DEFL=0.
   50  DO21J=1,N
       K=N-J+1
       DEFL=DEFL+F(J)*G(K)
       EPSTAR=EPSTAR+F(J)*E(K)
   21  EPS=EPS+F(J)*Z(K)
       EPS=EPS*CC
       EPSTAR=EPSTAR*CC
       EPSBAR=EPS*A2/H/V
   51  DEFL=DEFL*C
       ALPHA=SIGN(1.0,FNEW)*(ABS(FNEW)/K2)**S
       PRINT1000,N,T,FNEW,ALPHA,EPS,EPSTAR,EPSBAR,DEFL
  100  CONTINUE
       STOP
 1000  FORMAT(1X,I4,7(3X,F15.8))
       END
```

DI = .1000000E-02   M.E.I = .26939VE-02   M = .1000000E 00   K2 = .2400000E 12   DELTA = .1000000E-02   EI = .362860E 03

N	T	F(X)	ALPHA	STRAIN	AVER. STRAIN	NONDIM. STRAIN	DEFLECTION
1	.1000000E 06	.1150897E 03	.5990818E-06	.2680347E-07	.2601771E-07	.1002894E-04	.1781423E-09
2	.2000000E 06	.1522338E 03	.1199284E-05	.1474628E-06	.1432162E-06	.5517556E-04	.6686928E-09
3	.3000000E 06	.5785748E 03	.1797900E-05	.4472690E-06	.4345854E-06	.1673527E-03	.2090123E-08
4	.4000000E 06	.1410693E 04	.2395091E-05	.1014752E-05	.9864524E-06	.3796855E-03	.4884291E-08
5	.5000000E 06	.2990357E 04	.2990357E-05	.1935854E-05	.1882756E-05	.7243505E-03	.9593337E-08
6	.6000000E 06	.1027713E 04	.3583127E-05	.3291056E-05	.3202266E-05	.1231400E-02	.1678451E-07
7	.7000000E 06	.2045760E 04	.4172614E-05	.5153903E-05	.5017176E-05	.1928436E-02	.2704025E-07
8	.8000000E 06	.2491494E 04	.4750823E-05	.7590705E-05	.7392505E-05	.2601819E-02	.4095105E-07
9	.9000000E 06	.2962040E 04	.5340556E-05	.1046580E-04	.1038593E-04	.3985337E-02	.5911022E-07
10	.1000000E 07	.3454639E 04	.5917419E-05	.1441230E-04	.1404791E-04	.5392592E-02	.8210968E-07
11	.1100000E 07	.3966729E 04	.6488814E-05	.1889207E-04	.1842194E-04	.7067681E-02	.1105367E-06
12	.1200000E 07	.4496540E 04	.7054160E-05	.2413614E-04	.2354688E-04	.9030919E-02	.1449712E-06
13	.1300000E 07	.5041211E 04	.7612819E-05	.3017513E-04	.2944735E-04	.1129501E-01	.1859347E-06
14	.1400000E 07	.5598440E 04	.8164413E-05	.3703302E-04	.3615409E-04	.1385409E-01	.2341317E-06
15	.1500000E 07	.6167430E 04	.8706205E-05	.4473001E-04	.4368355E-04	.1673666E-01	.2899611E-06
16	.1600000E 07	.6744942E 04	.9243722E-05	.5327020E-04	.5205220E-04	.1993486E-01	.3540015E-06
17	.1700000E 07	.7329641E 04	.9770444E-05	.6269013E-04	.6126714E-04	.2345649E-01	.4267662E-06
18	.1800000E 07	.7919530E 04	.1028787E-04	.7296584E-04	.7133389E-04	.2730131E-01	.5087509E-06
19	.1900000E 07	.8512877E 04	.1079551E-04	.8410760E-04	.8253215E-04	.3146980E-01	.6004324E-06
20	.2000000E 07	.9107951E 04	.1129576E-04	.9610994E-04	.9401942E-04	.3596104E-01	.7022675E-06
21	.2100000E 07	.9703759E 04	.1177964E-04	.1089609E-03	.1066333E-03	.4077171E-01	.8146919E-06
22	.2200000E 07	.1029563E 05	.1225526E-04	.1226631E-03	.1200771E-03	.4597900E-01	.9381196E-06
23	.2300000E 07	.1048070E 05	.1271937E-04	.1371905E-03	.1343402E-03	.5133361E-01	.1072942E-05
24	.2400000E 07	.1147201E 05	.1317162E-04	.1525366E-03	.1494644E-03	.5704725E-01	.1217528E-05
25	.2500000E 07	.1205249E 05	.1361163E-04	.1686729E-03	.1652507E-03	.6311620E-01	.1372022E-05
26	.2600000E 07	.1262467E 05	.1403910E-04	.1855754E-03	.1818699E-03	.6943675E-01	.1549345E-05
27	.2700000E 07	.1318004E 05	.1445371E-04	.2032277E-03	.1992233E-03	.7040947E-01	.1731910E-05
28	.2800000E 07	.1374133E 05	.1445519E-04	.2215962E-03	.2172800E-03	.6291423E-01	.1930030E-05
29	.2900000E 07	.1428334E 05	.1524330E-04	.2400578E-03	.2360350E-03	.9045593E-01	.2140110E-05
30	.3000000E 07	.1481291E 05	.1561779E-04	.2603756E-03	.2544472E-03	.9742471E-01	.2363650E-05
31	.3100000E 07	.1532040E 05	.1597849E-04	.2807275E-03	.2754802E-03	.1050358E 00	.2600843E-05
32	.3200000E 07	.1583070E 05	.1632520E-04	.3016717E-03	.2961059E-03	.1128752E 00	.2851860E-05
33	.3300000E 07	.1632250E 05	.1665577E-04	.3231760E-03	.3172960E-03	.1207210E 00	.3115244E-05
34	.3400000E 07	.1680803E 05	.1697011E-04	.3452005E-03	.3399960E-03	.1294044E 00	.3591333E-05
35	.3500000E 07	.1725776E 05	.1725011E-04	.3677249E-03	.3619710E-03	.1375900E 00	.3689160E-05
36	.3600000E 07	.1754907E 05	.1756683E-04	.3906447E-03	.3638467E-03	.1461849E 00	.3996655E-05
37	.3700000E 07	.1609642E 05	.1744778E-04	.4140772E-03	.4091095E-03	.1543353E 00	.4184418E-05
38	.3800000E 07	.1684939E 05	.1810537E-04	.4378349E-03	.4303523E-03	.1638228E 00	.4545400E-05
39	.3900000E 07	.1688765E 05	.1835148E-04	.4619202E-03	.4541327E-03	.1723726E 00	.5004947E-05
40	.4000000E 07	.1922500E 05	.1858311E-04	.4863114E-03	.4782140E-03	.1819608E 00	.5369371E-05
41	.4100000E 07	.1954060E 05	.1880031E-04	.5109684E-03	.5025576E-03	.1911568E 00	.5748563E-05
42	.4200000E 07	.1980134E 05	.1900315E-04	.5358304E-03	.5271293E-03	.2004916E 00	.6141651E-05
43	.4300000E 07	.2017519E 05	.1919172E-04	.5608688E-03	.5518790E-03	.2096391E 00	.6548815E-05
44	.4400000E 07	.2040935E 05	.1936612E-04	.5859724E-03	.5767040E-03	.2192092E 00	.6969941E-05
45	.4500000E 07	.2070573E 05	.1952645E-04	.6113070E-03	.6017225E-03	.2287535E 00	.7404006E-05
46	.4600000E 07	.2094167E 05	.1967293E-04	.6367912E-03	.6268730E-03	.2382422E 00	.7853534E-05
47	.4700000E 07	.2115419E 05	.1980569E-04	.6621133E-03	.6521130E-03	.2474196E 00	.8315701E-05
48	.4800000E 07	.2134245E 05	.1992480E-04	.6875032E-03	.6750032E-03	.2572390E 00	.8791195E-05
49	.4900000E 07	.2151577E 05	.2003075E-04	.7128365E-03	.7021001E-03	.2672201E 00	.9279614E-05
50	.5000000E 07	.2166534E 05	.2012347E-04	.7381016E-03	.7272983E-03	.2761723E 00	.9781335E-05

57

```fortran
C          SMINE2 -- PLASTIC CONTACT LAW
C
COMPUTATION OF TIMOSHENKO"S SMALL INCREMENT SOLUTION OF HERTZIAN IMPACT
C                       OF A SIMPLE BEAM
C     DT - TIME INCREMENT
C     NDT - NO. OF TIME INCREMENTS CALCULATED
C     NH - NO. OF BEAM MODES CONSIDERED
C     TOL - TOLERANCE OF ERROR IN NONLINEAR SOLUTION
C     PR1, PR2 - POISSON"S RATIO OF BEAM, IMPACTOR
C     V - IMPACT VELOCITY
C     R1 - RADIUS OF IMPACTOR
C     FI - FLEXURAL RIGIDITY
C     H, B, L - THICKNESS, WIDTH, SPAN OF BEAM
C     RHO1, RHO2 - DENSITY OF BEAM, IMPACTOR
C     K2 - HERTZIAN CONTACT STIFFNESS
C     M1, M2 - MASS OF BEAM, IMPACTOR
      REAL L,M1,K2,KZERO,M
      LOGICAL PLAST
      DIMENSION F(5000),G(5000),Z(5000)
 1001 FORMAT(4X,"N",10X,"T",16X,"F(N)",14X,"ALPHA",12X,"STRAIN",
     1            8X,"NONDIM. STRAIN",5X,"DEFLECTION")
C        PROBLEM DATA
      NH=40
      NDT= 50
      TOL=1.0E-05
      DT=0.1E-06
      V=6.0
      M1=0.1
      M2=1.0
      E=2.10E11
      L=0.20
      H=0.012
      B=0.012
      FI=E*B*H**3/12.
C**********  PLASTIC CONTACT LAW   *************
      KZERO=9.0E 05
      FTA=0.5
C*****************************************************************************
      PI=3.14159265398
      PLAST=.TRUE.
      ALFSET=0.
      FNM1=0.
      M=M1/M2
      A2=SQRT(EI*L/M1)
      Q=1./3.
      S=2./3.
      PRINT1002,DT,A2,M,KZERO,EI
 1002 FORMAT("   DT = ",F13.6,"    A**2 = ",F13.6,"    M = ",E13.6,"    KZER
     10 = ",F13.6,"      FI =",E13.6)
      PRINT1001
      A=DT**2/3.0/M2
      C=2.0*L**3/(EI*PI**4)
      TERM1=PI**2*A2*DT/L**2
      DO 90 K=1,NDT
      Z(K)=0
 90   G(K)=0
      DO61=1,NH,2
      J=I**2
```

58

```
              TERM2=J*TERM1
              JJ=J**2
              C2=1.0
              DO6K=1,NDT
              C1=C2
              C2=COS(K*TERM2)
              TERM=C1-C2
```
CREATE TABLE OF SUMMATION FUNCTIONS
```
              Z(K)=Z(K)+TERM/J
         6    G(K)=G(K)+TERM/JJ
              P=B+C*G(1)
```
COLUMN HEADINGS
```
              DO100N=1,NDT
              IF(MOD(N,59).NE.0)GOTO70
              PRINT1003
       1003   FORMAT(1H1)
              PRINT1001
```
CALCULATE TERMS IN NONLINEAR EQUATION IN F(N)
```
         70   T=N*DT
              A=V*T
              IF(N.EQ.1)GOTO14
              SUM=0.
              SUMI=0.
              RUM=0.
              NM1=N-1
              DO5J=1,NM1
              K=N-J
              R=K
              SUMI=F(J)-SUMI
              SUM=SUM+R*SUMI
         5    RUM=RUM+F(J)*G(K+1)
              A=A-C*RUM
              A=A-DT**2*(2.*SUM-SUMI/3.)/M2
```
COMPUTE SOLUTION FOR F(N)
```
              IF(PLAST)GOTO14
              GOTO62
         14   FNEW=(A-ALFSET)/(P+1.0/KZERO)
              ALPHA=ALFSET+FNEW/KZERO
              IF(FNEW.GT.0.)GOTO60
              F(N)=0.
              GOTO61
         60   IF(FNEW.GT.FNM1)GOTO64
              PLAST=.FALSE.
              ALPHAM=ALPHA
              FM=FNEW
              GOTO64
         62   A=A-ALPHAM*ETA
         63   FN=FNEW
              B=SIGN(1.0,FN)*(ALPHAM*(1.0-ETA))**3/FM**2-3.0*A*P**2
              FFN=P**3*FN**3+B*FN**2
        1     +3.0*A**2*P*FN-A**3
              FPFN=3.0*P**3*FN**2+2.0*B*FN+3.0*A**2*P
         82   FNEW=FN-FFN/FPFN
              ERROR=ABS((FNEW-FN)/FN)
              IF(ERROR.GT.TOL)GOTO63
              IF(FNEW.GT.0.)GOTO65
              PLAST=.TRUE.
              ALPHA=ALPHAM*ETA
```

59

```
      ALFSFT=ALPHA
      F(N)=0.
      GOTO61
   65 ALPHA=ALPHAM*(ETA+(1.0-ETA)*(FNEW/FM)**S)
   64 F(N)=FNEW
   61 FNM1=FNEW
CALCULATE DEFLECTION AND STRAIN
      FPS=0.
      DEFL=0.
   50 DO21J=1,N
      K=N-J+1
      DEFL=DEFL+F(J)*G(K)
   21 FPS=FPS+F(J)*Z(K)
      FPS=FPS*L*H/EI/PI**2
      FPSBAR=EPS*A2/H/V
   51 DEFL=DEFL*2.0*L**3/EI/PI**4
      PRINT1000,N,T,FNEW,ALPHA,EPS,EPSBAR,DEFL
  100 CONTINUE
      STOP
 1000 FORMAT(1X,I4,6(3X,F15.8))
      END
```

60

DT = .100000E-06   A**2 = .269399E 02   M = .100000E 00   KZERO = .900000E 06   EI = .362880E 03

N	T	F(N)	ALPHA	STRAIN	NONDIM. STRAIN	DEFLECTION
1	.1000000E-06	.53999844E 00	.59999871E-06	.15102403E-08	.56508017E-06	.12910026E-11
2	.2000000E-06	.10799947E 01	.11999941E-05	.60800617E-08	.22749506E-05	.58754562E-11
3	.3000000E-06	.16199967E 01	.17999852E-05	.12927031E-07	.48308520E-05	.14727796E-10
4	.4000000E-06	.21599744E 01	.23999715E-05	.20959340E-07	.78421547E-05	.28392277E-10
5	.5000000E-06	.26999570E 01	.29999523E-05	.30208049E-07	.11302817E-04	.47584205E-10
6	.6000000E-06	.32399341E 01	.35992268E-05	.40982656E-07	.15334301E-04	.72993487E-10
7	.7000000E-06	.37799051E 01	.41998945E-05	.52970059E-07	.19819581E-04	.10511602E-09
8	.8000000E-06	.43198296E 01	.47998551E-05	.65805049E-07	.24621925E-04	.14436402E-09
9	.9000000E-06	.48598272E 01	.53980800E-05	.79630959E-07	.29795177E-04	.19126536E-09
10	.1000000E-05	.53997774E 01	.59997522E-05	.94586078E-07	.35390370E-04	.24630063E-09
11	.1100000E-05	.59397199E 01	.65996880E-05	.11042155E-06	.41315962E-04	.30983685E-09
12	.1200000E-05	.64796544E 01	.71996160E-05	.12696475E-06	.47507357E-04	.38223295E-09
13	.1300000E-05	.70195805E 01	.77995339E-05	.14438637E-06	.54025182E-04	.46391953E-09
14	.1400000E-05	.75594786E 01	.83994206E-05	.16272853E-06	.60887941E-04	.55528376E-09
15	.1500000E-05	.80993460E 01	.89934060E-05	.18177293E-06	.68013201E-04	.65662613E-09
16	.1600000E-05	.86393049E 01	.95992272E-05	.20145694E-06	.75382604E-04	.76827360E-09
17	.1700000E-05	.91791941E 01	.10199105E-04	.22193724E-06	.83041311E-04	.89060250E-09
18	.1800000E-05	.97190733E 01	.10728970E-04	.24319027E-06	.90994652E-04	.10239334E-08
19	.1900000E-05	.10258942E 02	.11398825E-04	.26505134E-06	.99173129E-04	.11685298E-08
20	.2000000E-05	.10798801E 02	.11988646E-04	.28750346E-06	.10757395E-03	.13246987E-08
21	.2100000E-05	.11338648E 02	.12598498E-04	.31069487E-06	.11625194E-03	.14927764E-08
22	.2200000E-05	.11878485E 02	.13198317E-04	.33456301E-06	.12518201E-03	.16730353E-08
23	.2300000E-05	.12418310E 02	.13798123E-04	.35894398E-06	.13430454E-03	.18657158E-08
24	.2400000E-05	.12958124E 02	.14397916E-04	.38390287E-06	.14364330E-03	.20711122E-08
25	.2500000E-05	.13497926E 02	.14997696E-04	.40955790E-06	.15324253E-03	.22895274E-08
26	.2600000E-05	.14037716E 02	.15597464E-04	.43579701E-06	.16306031E-03	.25211964E-08
27	.2700000E-05	.14577493E 02	.16197215E-04	.46249477E-06	.17304970E-03	.27663459E-08
28	.2800000E-05	.15117257E 02	.16726954E-04	.48976360E-06	.18325276E-03	.30252615E-08
29	.2900000E-05	.15657011E 02	.17396679E-04	.51768956E-06	.19370170E-03	.32982167E-08
30	.3000000E-05	.16196750E 02	.17996389E-04	.54611843E-06	.20433081E-03	.35854153E-08
31	.3100000E-05	.16736476E 02	.18596085E-04	.57496627E-06	.21513268E-03	.38870772E-08
32	.3200000E-05	.17276189E 02	.19195191E-04	.60439191E-06	.22619256E-03	.42034834E-08
33	.3300000E-05	.17815808E 02	.19795431E-04	.63443690E-06	.23738455E-03	.45348783E-08
34	.3400000E-05	.18355573E 02	.20395082E-04	.66495537E-06	.24878411E-03	.48814383E-08
35	.3500000E-05	.18895245E 02	.20994710E-04	.69576585E-06	.26033174E-03	.52438338E-08
36	.3600000E-05	.19434902E 02	.21594435E-04	.72722577E-06	.27212297E-03	.56209944E-08
37	.3700000E-05	.19974544E 02	.22193938E-04	.75926963E-06	.28409268E-03	.60144838E-08
38	.3800000E-05	.20514172E 02	.22793625E-04	.79184758E-06	.29620740E-03	.64240014E-08
39	.3900000E-05	.21053782E 02	.23393095E-04	.82440018E-06	.30846230E-03	.68497763E-08
40	.4000000E-05	.21593383E 02	.23992648E-04	.85780105E-06	.32095760E-03	.72920380E-08
41	.4100000E-05	.22132960E 02	.24592185E-04	.89175257E-06	.33363265E-03	.77511305E-08
42	.4200000E-05	.22672534E 02	.25191700E-04	.92591958E-06	.34644738E-03	.82270023E-08
43	.4300000E-05	.23212058E 02	.25791200E-04	.96044015E-06	.35936300E-03	.87199587E-08
44	.4400000E-05	.23751621E 02	.26390690E-04	.99571260E-06	.37250135E-03	.92303087E-08
45	.4500000E-05	.24291141E 02	.26990157E-04	.10315353E-05	.38596510E-03	.97581832E-08
46	.4600000E-05	.24830642E 02	.27589600E-04	.10673600E-05	.39937920E-03	.10303635E-07
47	.4700000E-05	.25370134E 02	.28189037E-04	.11034940E-05	.41289960E-03	.10866941E-07
48	.4800000E-05	.25909604E 02	.28788449E-04	.11405433E-05	.42675244E-03	.11448489E-07
49	.4900000E-05	.26449058E 02	.29387843E-04	.11763453E-05	.44088520E-03	.12048340E-07
50	.5000000E-05	.26938495E 02	.29987218E-04	.12158670E-05	.45943270E-03	.12666527E-07

61
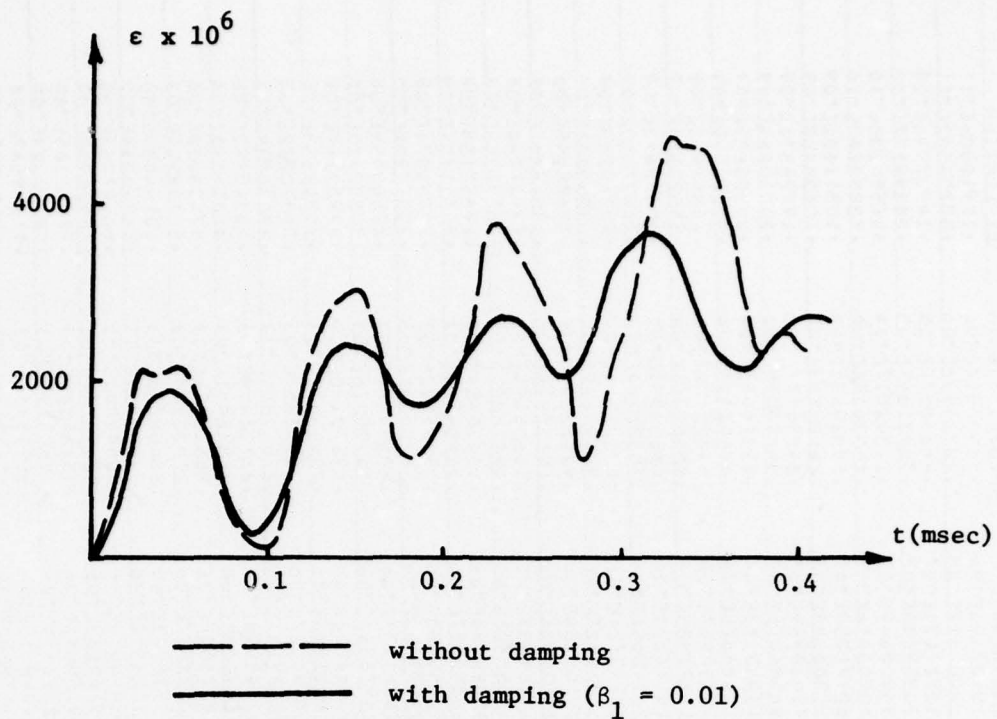
Figure B1. Comparison of midspan bending strain calculated by Timoshenko small-increment method with and without internal damping. (Aluminum beam, 152x20x12.7 mm; steel impactor, 0.110 kg; v = 6.19 m/sec; M = 0.998).

Figure B2. Plastic Contact Law.

62

Figure B3. Complication of plastic contact law caused by
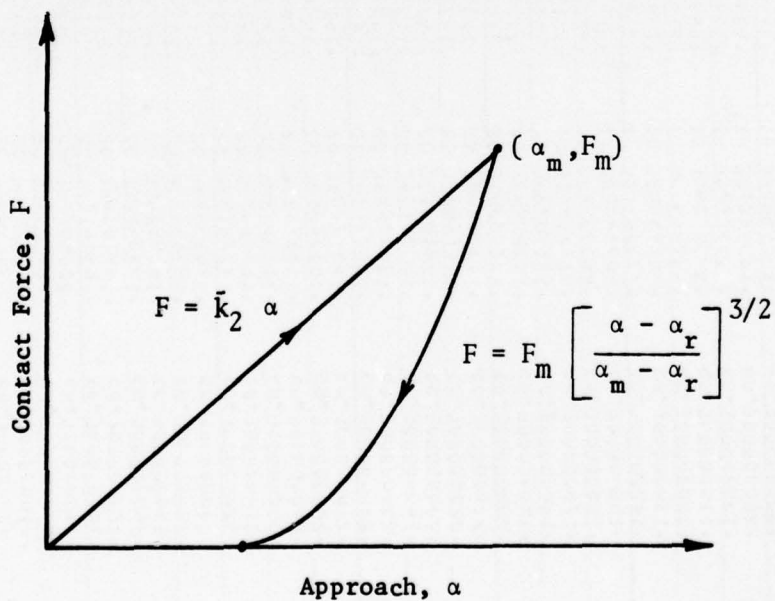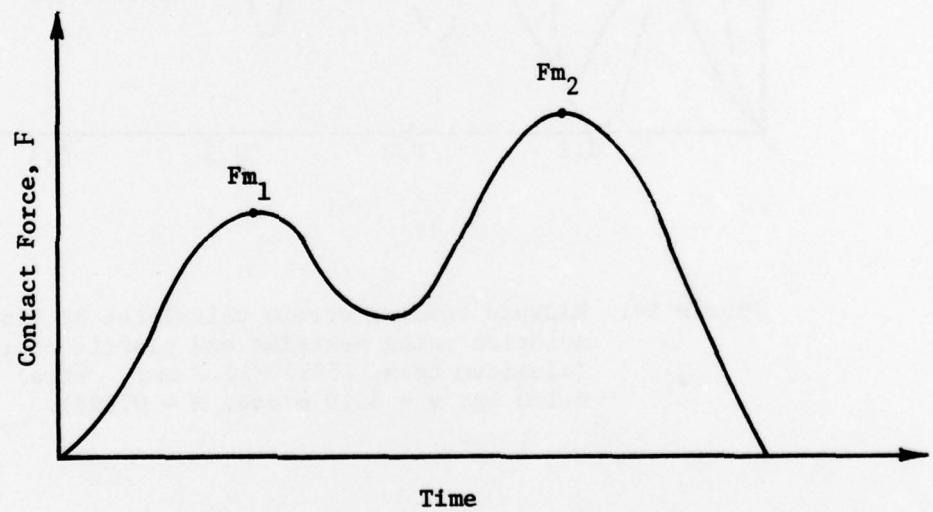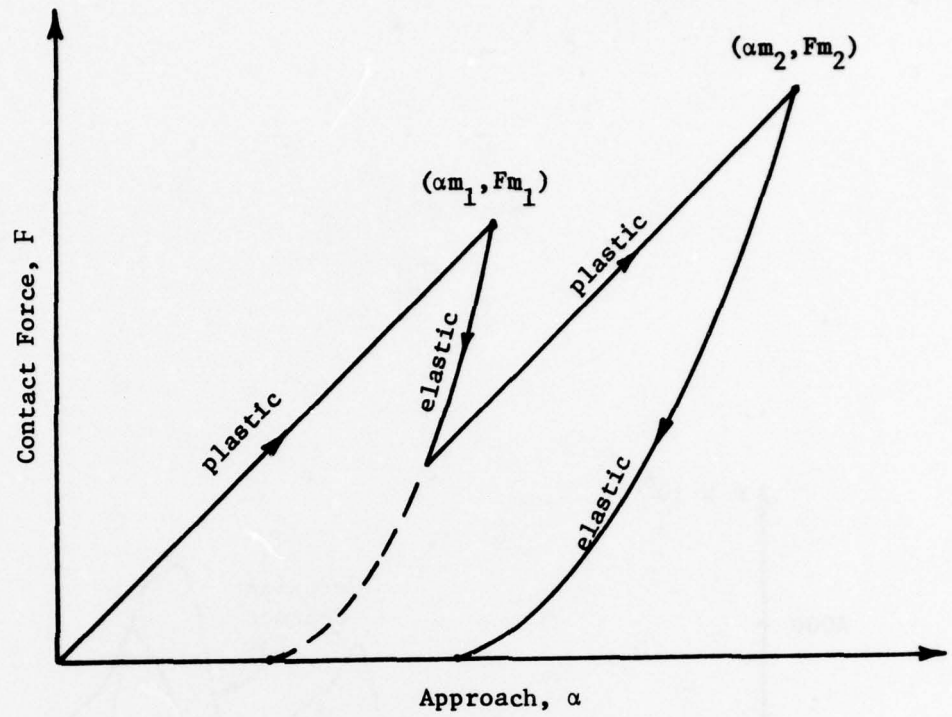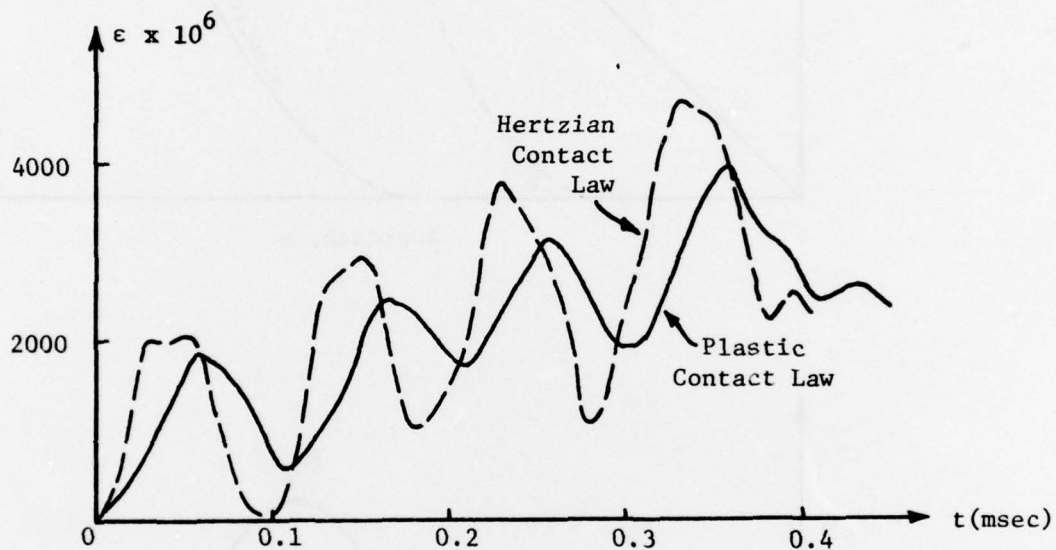second increase in contact force during a single
sub-impact.

63

Figure B4. Midspan bending strain calculated by Timoshenko solution using Hertzian and plastic contact laws. (Aluminum beam, 152x20x12.7 mm; steel impactor, 0.110 kg; v = 6.19 m/sec; M = 0.998).

64

Appendix C – Impact-to-Failure Experiments of Composite Beams

In addition to the strain-measurement impact experiments described in
the main text, a series of tests were conducted in which laminated composite
beams were impacted to failure. This appendix presents the details of these
experiments and demonstrates the construction of an impact design curve for
a particular structure by using experimental data alone.

Specimens

All specimens were fabricated from Hercules, Inc., type AS3501 graphite-
epoxy prepreg tape. Specimen dimensions, lamination lay-ups, and other data
are summarized in Table C1. The flexural rigidities listed in the table were
determined from static three-point bending tests, as described in the main text.

Experimental Procedure

In each impact-to-failure test, a simply supported graphite-epoxy com-
posite beam was repeatedly impacted by the same mass projected from an air
gun at gradually increasing velocities until failure of the specimen was
detected by visual inspection. Impact velocity was measured using the photo-
graphic technique described in section III of the main text. Experiments were
performed on several specimens of the same type, i.e., same dimensions and
lay-up.

The average of the highest impact velocity, v_d, for which a particular
type of specimen did not fail, and the lowest velocity, v_f, for which any
failure was detected, is regarded as the critical or failure velocity,

$$v_c = \frac{v_d + v_f}{2} .$$ \hfill (C1)

65

This velocity is used in characterizing the impact resistance of each type of specimen for a particular impact mass (see Table C2).

In several cases, the no-failure velocity v_d for a specimen was greater than the failure velocity v_f for another specimen of the same type; i.e., some specimens were more impact resistant than other similar specimens. Such expected "scatter" in impact resistance was not large, however, and no special steps are taken to account for it in the table.

Failure Modes

In specimens which were only slightly damaged by the impact, the damage almost exclusively consisted of rupture of the beam surface opposite the impact point. This was accompanied in more damaged specimens by breakage of the impacted surface and by delamination. Apparently, the predominant mode of initial failure was tensile fiber breakage on the surface opposite the impact point.

Construction of Design Curve

The generalized strain associated with each of these failure impact cases has been calculated according to the formula

$$\bar{\varepsilon}_f = \varepsilon_f \frac{a^2}{hv_c} \tag{C2}$$

where ε_f is the surface-ply strain at beam failure for each specimen type. We shall adopt the maximum strain failure theory; i.e., failure occurs when the strain in the fiber direction of a ply reaches a critical value, taken here as 0.0112. Since the surface plies of our laminates are not oriented at 0°, initial failure does not occur on the surface, but occurs in the outermost 0° plies. The value 0.0112 for the flexural failure strain was published by the material manufacturer (Hercules Product Data Sheet No. 832).

An impact design curve may be constructed by plotting the experimental data as points on an $\bar{\epsilon}$ vs. M graph (Fig. C1). Note that these points are very close to a curve representing the one-degree-of-freedom energy-conserved impact model described in the main text. This may be a mere coincidence.

The fact that the experimental points can be approximately represented as a single curve suggests that, for a particular type of structure, only one impact-to-failure experiment may be required to construct a complete design curve. That is, only one test is necessary to fix a point, through which the curve may be drawn as a straight line on a log-log plot of $\bar{\epsilon}_f$ vs. M. The single test determines the value of the constant C in the design curve equation

$$\bar{\epsilon}_f = \frac{C}{\sqrt{M}} \qquad (C3)$$

Alternate Design Curve

The design curve of Fig. 5 in terms of $\bar{\epsilon}$ vs. M gives the maximum strain in the beam for a given impact situation. For the impact-to-failure experiment, the failure strain is assumed known, and the design curve of Fig. C1 tells us under what impact condition this failure stress will be reached. For this purpose, it is desirable to plot Fig. C1 in terms of a dimensionless impact velocity $\bar{v}$, defined as

$$\bar{v} = v \frac{h}{a^2 \epsilon_f} \qquad (C4)$$

which is the reciprocal of $\bar{\epsilon}$, but with ϵ_f used as ϵ. For a given value of M, the beam will not fail at small values of v or $\bar{v}$. As v, or $\bar{v}$, is increased to the value v_c, or $\bar{v}_c$, failure will occur, where v_c and $\bar{v}_c$ are related by

$$\bar{v}_c = v_c \frac{h}{a^2 \epsilon_f} = \frac{1}{\bar{\epsilon}_f} \qquad (C5)$$

67

Fig. (C2) shows the experimental test points in terms of $\bar{v}_c$ vs. M, which again can be approximated by one curve. This curve divides the plane into two regions, an unsafe region above the curve and a safe region below. With this curve, the designer can conveniently determine, for a given impactor mass m_2, what maximum velocity v_c the beam can withstand.

68

Table C1   Impact-to-Failure Test Specimens

Specimen Type	Average Dimensions, Lxbxh (mm) and Lay-up	Supported Mass, m_l (kg)	Flexural Rigidity, EI (N-m^2)	Static Surface-ply strain at beam failure, ε_f *
A	76.2x36.8x1.57 $[\pm 45/0_2/\mp 45]_2$	0.00617	0.571	0.0168
B	76.2x37.1x1.80 $[\pm 45/0_2/\mp 45]_2$	0.00702	0.799	0.0168
C	152.4x76.7x2.62 $[\pm 45/0_2/\mp 45]_3$	0.0424	5.63	0.0144
D	152.4x76.8x3.57 $[\pm 45/0_2/\mp 45]_4$	0.0578	15.55	0.01344

* Note: Beam failure is assumed to occur in the outermost 0° layer when its longitudinal strain reaches 0.0112.

69

Table C2   Impact-to-Failure Test Data

| Specimen Type (see Table C1) | Impactor mass, m_2 (kg) | Mass ratio, $M=m_1/m_2$ | Impact Velocity (m/sec) | | | Generalized strain, $\bar{\epsilon} = \epsilon_f \dfrac{a^2}{hv_c}$ |
			Highest no-fail velocity, v_d	Lowest velocity at which specimen failed, v_f	Critical velocity, $v_c=(v_d+v_f)/2$	
A	0.1095	0.0562	7.91	8.26	8.08	3.47
	0.0566	0.1089	11.27	11.47	11.37	2.47
	0.0280	0.220	17.6	19.2	18.4	1.526
	0.01434	0.429	22.0	22.7	22.3	1.25β
B	0.1095	0.0639	7.83	9.61	8.72	3.15
	0.0566	0.1238	9.21	10.75	9.98	2.76
	0.0280	0.250	14.0	13.15	13.58	2.02
	0.01434	0.488	17.2	25.7	21.4	1.28
C	0.1095	0.386	13.8	16.5	15.1	1.631
	0.0566	0.748	20.2	25.0	22.6	1.094
	0.0280	1.510	28.6	33.2	30.9	0.799
	0.01434	2.95	38.8	37.5	38.1	0.648
D	0.1095	0.527	16.0	17.8	16.9	1.426
	0.0566	1.02	21.3	23.5	22.4	1.074
	0.0280	2.06	36.1	38.6	37.3	0.646
	0.01434	4.02	38.8	44.5	41.7	0.578
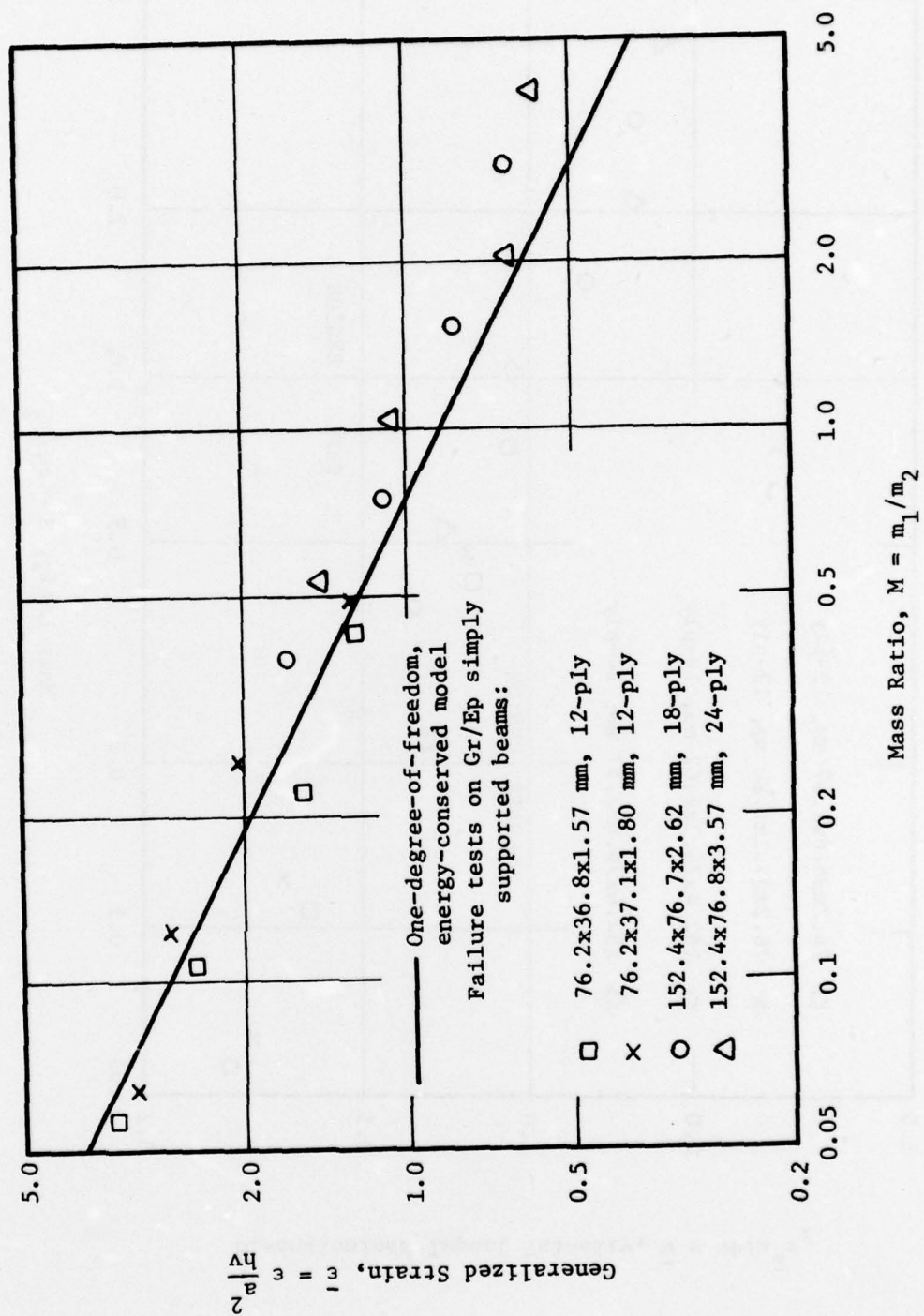
Figure C1. Design Curve as Determined by Experiment.

71

Figure C2. Alternate Presentation of Design Curve
Showing Impact-to-Failure Experiment Data
for Graphite-Epoxy Laminated Beams

72

DISTRIBUTION LIST

Government Activities

<table>
<tr><td></td><td>No. of
Copies</td></tr>
</table>

NAVAIRSYSCOM, AIR-954 (2 for retention), 2 for AIR-530,
   1 for AIR-320B, AIR-52032D, AIR-5302, AIR-53021, AIR-530215). .   9
NAVSEASYSCOM, Washington, D. C. 20362
   (Attn: Code 035, Mr. C. Pohler). 1
NAVSEC, Hyattsville, MD 20782
   (Attn: Code 6101E03, Mr. W. Graner). 1
ONR, Washington, D. C. 20362
   (Attn: Dr. N. Perrone) 1
NAVSHIPRANDCEN, Bethesda, MD 20034
   (Attn: Code 173.2, Mr. W. P. Cauch). 1
NAVSHIPRANDCEN, Annapolis, MD 21402
   (Attn: Code 2870, Mr. H. Edelstein). 1
NOL, White Oak, MD 20910
   (Attn: Mr. F. R. Barnet). 1
NRL, Washington, D. C. 20375
   (Attn: Dr. I. Wolock). 1
NAVPGSCHL, Monterey, CA 95940
   (Attn: Prof. R. Ball, Prof M. H. Bank) 2
AFOSR, Washington, D. C. 20333
   (Attn: Mr. J. Pomerantz) 1
AFML, WPAFB, OH 45433
   (Attn: LAM (Technical Library)). 1
   (Attn: LT-1/Mr. W. R. Johnston). 1
   (Attn: LTF/Mr. T. Cordell) 1
   (Attn: FBSC/Mr. L. Kelly). 1
   (Attn: MAC/Mr. G. P. Peterson) 1
   (Attn: MXA/Mr. F. J. Fechek) 1
   (Attn: MBC/Mr. T. G. Reinhard, Jr) 1
AFFDL, WPAFB, OH 45433
   (Attn: FB/Mr. P. A. Parmley) 2
   (Attn: FBC/Mr. C. Wallace) 1
   (Attn: FBC/Mr. E. E. Zink) 1
USAMATCOM, Research Div., Washington, D.C. 20315
   (Attn: Mr. D. J. Jones). 1
USAMATRESAG, Watertown, MA
   (Attn: Dr. E. Lenoe) 1
USARESOFC, Durham, MC 27701 1
USAAVMATLAB, Fort Eustis, VA 23603
   (Attn: Mr. R. Beresford). 1
PLASTEC, Picatinny Arsenal, Dover, NJ 07801
   (Attn: Librarian, Bldg. 176, SARPA-FR-M-D and Mr. H. Pebly). . 2
NASA (ADM), Washington, D.C. 20546
   (Attn: Secretary). 1

General Dynamics/Convair, San Diego, CA 92138
    (Attn: Mr. D. R. Dunbar, W. G. Scheck) 2
General Dynamics, Fort Worth, TX 76101
    (Attn: Mr. P. D. Shockey, Dept. 23, Mail Zone P-46). 1
General Electric Company, Phila., PA 19101
    (Attn: Mr. L. McCreight) 1
Great Lakes Carbon Corp., N.Y., NY 10017
    (Attn: Mr. W. R. Benn, Mgr., Markey Development) 1
Grumman Aerospace Corporation, Bethpage, L.I., NY 11714
    (Attn: Mr. R. Hadcock, Mr. S. Dastin). 2
Hercules Powder Company, Inc., Cumberland, MD 21501
    (Attn: Mr. D. Hug) 1
H. I. Thompson Fiber Glass Company, Gardena, CA 90249
    (Attn: Mr. N. Myers) 1
ITT Research Institute, Chicago, IL 60616
    (Attn: Dr. R. Cornish) 1
J. P. Stevens & Co., Inc., N.Y., NY 10036
    (Attn: Mr. H. I. Shulock). 1
Kaman Aircraft Corporation, Bloomfield, CT 06002
    (Attn: Tech. Library). 1
Lehigh University, Bethlehem, PA 18015
    (Attn: Dr. G. C. Sih). 1
Lockheed-California Company, Burbank, CA 91520
    (Attn: Mr. E. K. Walker, R. L. Vaughn) 2
Lockheed-Georgia Company, Marietta, GA
    (Attn: Advanced Composites Information Center, Dept. 72-14,
            Zone 42). 1
LTV Aerospace Corporation, Dallas, TX 75222
    (Attn: Mr. O. E. Dhonau/2-53442, C. R. Foreman). 2
Martin Company, Baltimore, MD 21203
    (Attn: Mr. J. E. Pawken) 1
Materials Sciences Corp., Blue Bell, PA 19422 1
McDonnell Douglas Corporation, St. Louis, MO 63166
    (Attn: Mr. R. C. Goran, O. B. McBee, C. Stenberg). 3
McDonnell Douglas Corporation, Long Beach, CA 90801
    (Attn: H. C. Schjelderup, G. Lehman) 2
Minnesota Mining and Manufacturing Company, St. Paul, MN 55104
    (Attn: Mr. W. Davis) 1
Northrop Aircraft Corp., Norair Div., Hawthorne, CA 90250
    (Attn: Mr. R. D. Hayes, J. V. Noyes, P. E. Lee). 3
Rockwell International, Columbus, OH 43216
    (Attn: Mr. O. G. Acker, K. Clayton). 2
Rockwell International, Los Angeles, CA 90053
    (Attn: Dr. L. Lackman) 1
Rockwell International, Tulsa, OK 74151
    (Attn: Mr. E. Sanders, Mr. J. H. Powell) 2
Owens Corning Fiberglass, Granville, OH 43023
    (Attn: Mr. D. Mettes). 1

Rohr Corporation, Riverside, CA 92503
    (Attn: Dr. F. Riel and Mr. R. Elkin) 2
Ryan Aeronautical Company, San Diego, CA 92112
    (Attn: Mr. R. Long). 1
Sikorsky Aircraft, Stratford, CT 06497
    (Attn: Mr. J. Ray) 1
Southwest Research Institute, San Antonio, TX 78206
    (Attn: Mr. G. C. Grimes) 1
University of Oklahoma, Norman, OK 93069
    (Attn: Dr. G. M. Nordby) 1
Union Carbide Corporation, Cleveland, OH 44101
    (Attn: Dr. H. F. Volk) 1